Multi-objective Operation Management of a Renewable Micro Grid with Back-up Micro Turbine/Fuel Cell/Battery Hybrid Power Source

Anvari-Moghaddam, Amjad; Seifi, Alireza; Niknam, Taher; Alizadeh Pahlavani, Mohammadreza

Published in:
Energy

Publication date:
2011

Energy 36 (2011) 6490–6507

Contents lists available at SciVerse ScienceDirect

Energy

journal homepage: www.elsevier.com/locate/energy

Multi-objective operation management of a renewable MG (micro-grid) with back-up micro-turbine/fuel cell/battery hybrid power source

Amjad Anvari Moghaddam [a], Alireza Seifi [a], Taher Niknam [b,*], Mohammad Reza Alizadeh Pahlavani [c]

[a] Department of Power & Control, School of Electrical and Computer engineering, Shiraz University, Engineering Faculty No.1, Zand St., Shiraz, Iran
[b] Department of electrical and electronics engineering, Shiraz University of Technology, Shiraz, Iran
[c] Department of Electrical Engineering, Iran University of Science and Technology (IUST), Tehran, Iran

ARTICLE INFO

Article history:
Received 14 March 2011
Received in revised form
6 September 2011
Accepted 10 September 2011
Available online 14 October 2011

Keywords:
PSO (Particle swarm optimization)
Chaotic search
Multi-operation management
Micro-grid
RESs (Renewable energy sources)

ABSTRACT

As a result of today's rapid socioeconomic growth and environmental concerns, higher service reliability, better power quality, increased energy efficiency and energy independency, exploring alternative energy resources, especially the renewable ones, has become the fields of interest for many modern societies. In this regard, MG (Micro-Grid) which is comprised of various alternative energy sources can serve as a basic tool to reach the desired objectives while distributing electricity more effectively, economically and securely. In this paper an expert multi-objective AMPSO (Adaptive Modified Particle Swarm Optimization algorithm) is presented for optimal operation of a typical MG with RESs (renewable energy sources) accompanied by a back-up Micro-Turbine/Fuel Cell/Battery hybrid power source to level the power mismatch or to store the surplus of energy when it's needed. The problem is formulated as a nonlinear constraint multi-objective optimization problem to minimize the total operating cost and the net emission simultaneously. To improve the optimization process, a hybrid PSO algorithm based on a CLS (Chaotic Local Search) mechanism and a FSA (Fuzzy Self Adaptive) structure is utilized. The proposed algorithm is tested on a typical MG and its superior performance is compared to those from other evolutionary algorithms such as GA (Genetic Algorithm) and PSO (Particle Swarm Optimization).

1. Introduction

In recent years, the application of alternative energy sources such as wind, biomass, solar, hydro and etc. has become more widespread mainly due to needs for better reliability, higher power quality, more flexibility, less cost and smaller environmental footprints. On the other hand, DGs (Distributed Generations) such as PV (photovoltaics), micro-turbines, fuel cells and storage devices are expected to play an important role in future electricity supply and low carbon economy [1,2]. However, high penetration of DGs into the grid environment will bring new challenges for the safe and efficient power system operation. These challenges can be partially addressed by MG (Micro-Grid) which is defined as an aggregation of DGs, electrical loads and generation interconnected among themselves and with distribution network as well [2–5]. In this regard, the methodologies applied to manage and control the operation of MGs are going through continuous changing in order to make these networks optimized and active systems, therefore there is a strong need for more precise scheduling of energy sources in MGs considering different objectives.

So far, numerous scientific works have been developed by researchers dealt with the optimal operation scheduling under different loading conditions and objectives. At first, conventional economic scheduling has been proposed as a solution for the optimization problem through finding an optimal set of generators to satisfy load demand and operational constraints in an economical manner [6–8]. Due to the environmental concerns and pollutants emission from traditional fossil fuel units, single-objective optimization could no longer be satisfactory in the mentioned problem. To involve emission as a separate goal, multi-objective optimization techniques have been developed in articles in order to choose a definite number of units for supplying the load under a certain condition taking into account minimum levels of cost and emission for grid operation [9–13]. Recently, evolutionary algorithms such as GA (Genetic Algorithm), PSO (Particle Swarm Optimization) and so on have been increasingly proposed for solving the optimization problem because of their inherent nonlinear mapping, simplicity and powerful search capabilities [13–18]. Hybrid approaches such as Fuzzy-based evolutionary

* Corresponding author. Tel.: +98 711 2337852; fax: +98 711 6473575.
E-mail addresses: am.anvari@ieee.org (A.A. Moghaddam), seifi@shirazu.ac.ir (A. Seifi), taher_nik@yahoo.com, niknam@sutech.ac.ir (T. Niknam).

0360-5442/$ – see front matter © 2011 Elsevier Ltd. All rights reserved.
doi:10.1016/j.energy.2011.09.017

Nomenclature

X vector of the optimization variables
n total number of optimization variables
T total number of hours
N_g total number of generation units
N_s total number of storage units
N_k total number of load levels
$u_i(t)$ status of unit i at hour t
$P_{Gi}(t)$ active power output of ith generator at time t
$P_{sj}(t)$ active power output of jth storage at time t
$P_{\mathrm{Grid}}(t)$ active power bought/sold from/to the utility at time t
$B_{Gi}(t)$ bid of the ith DG source at hour t
$B_{sj}(t)$ bid of the jth storage options at hour t
$B_{\mathrm{Grid}}(t)$ bid of utility at hour t
S_{Gi} start-up/shut-down costs for ith DG unit
S_{sj} start-up/shut-down costs for jth storage device
$E_{Gi}(t)$ emissions in kg MW h^{-1} for ith DG unit at hour t
$E_{sj}(t)$ emissions in kg MW h^{-1} for jth storage device at hour t
$E_{\mathrm{Grid}}(t)$ emissions in kg MW h^{-1} for utility at hour t
$CO_{2_{DG_i}}(t)$ carbon dioxide pollutants of ith DG unit at hour t
$SO_{2_{DG_i}}(t)$ sulfur dioxide pollutants of ith DG unit at hour t
$NO_{x_{DG_i}}(t)$ nitrogen oxide pollutants of ith DG unit at hour t
$CO_{2_{Storage_j}}(t)$ carbon dioxide pollutants of jth storage device at hour t
$SO_{2_{Storage_j}}(t)$ sulfur dioxide pollutants of jth storage device at hour t
$NO_{x_{Storage_j}}(t)$ nitrogen oxide pollutants of jth storage device at hour t
$CO_{2_{Grid}}(t)$ carbon dioxide pollutants of utility at hour t
$SO_{2_{Grid}}(t)$ sulfur dioxide pollutants of utility at hour t
$NO_{x_{Grid}}(t)$ nitrogen oxide pollutants of utility at hour t
P_{Lk} the amount of kth load level
$P_{G,\min}(t)$ minimum active power production of ith DG at hour t
$P_{s,\min}(t)$ minimum active power production of jth storage at hour t
$P_{\mathrm{grid},\min}(t)$ minimum active power production of the utility at hour t
$P_{G,\max}(t)$ maximum active power production of ith DG at hour t
$P_{s,\max}(t)$ maximum active power production of jth storage at hour t
$P_{\mathrm{grid},\max}(t)$ maximum active power production of the utility at hour t
$W_{\mathrm{ess},t}$ battery energy storage at time t
$P_{\mathrm{Charge}}(P_{\mathrm{discharge}})$ permitted rate of charge (discharge) through a definite period of time
$\eta_{\mathrm{charge}}(\eta_{\mathrm{discharge}})$ charge (discharge) efficiency of the battery
$W_{\mathrm{ess,min}}(W_{\mathrm{ess,max}})$ lower (upper) bounds on battery energy storage
$P_{\mathrm{charge,max}}(P_{\mathrm{discharge,max}})$ maximum rate of charge (discharge) during each time interval
ω inertia weight
C_1, C_2 weighting factors of the stochastic acceleration terms (Learning factors)
rand $(\cdot)$ random function in the range of [0,1]
$P_{\mathrm{best}\ i}$ best previous experience of the ith particle that is recorded
G_{best} best particle among the entire population
F vector of objective functions
$f_i(X)$ ith objective function
$g_i(X)$ equality constraints of ith objective function
$h_i(X)$ inequality constraints of ith objective function
V_i^{k+1} updated velocity vector of ith particle
X_i^{k+1} updated position of ith particle
cx_i^j the jth chaotic variable
N_{choas} number of individuals for CLS
X_{cls}^0 initial population for CLS
N_{Swarm} number of the swarms
$\Delta\omega$ weight correction value
NBF Normalized Best Fitness
$\mathrm{BF}_{\min}$ minimum fitness value
$\mathrm{BF}_{\max}$ maximum fitness value

List of abbreviations

AMPSO Adaptive Modified Particle Swarm Optimization
FSAPSO Fuzzy Self Adaptive PSO
CPSO Chaotic Particle Swarm Optimization
DG Distributed Generation
DER Distributed Energy Resource
RES Renewable Energy Source
MG Micro-grid
MGCC (μ_{cc}) Micro-grid Central Controller
CLS Chaotic Local Search
WT Wind Turbine
PV Photovoltaic
PAFC Phosphoric Acid Fuel Cell
NiMH-Battery Nickel-Metal-Hydride Battery
MT Micro-Turbine

algorithms have been also used in scientific literatures many times [19–22]. Similarly, taking a comprehensive look at power dispatch techniques considering ON/OFF states of generation units shows that different optimization methods have been proposed to solve the mentioned problem [23–30]. Among these methods, Senjyu et al. [23] has used a priority list approach for handling the dispatch problem. Although such method saves the time, it gives schedules with relatively higher operation cost. Similarly, BB (Branch-and-Bound) method [24,25] may have some deficiencies handling large-scale problems. LR (Lagrangian Relaxation) method [27–30] focuses on finding an appropriate co-ordination technique for generating feasible primal solutions, while minimizing the duality gap. On the other hand, meta-heuristic methods (e.g., TS (Tabu Search), EP (Evolutionary Programming), SA (simulated annealing), and so on) are iterative techniques that are frequently used in optimal power dispatch problems [31–35]. Such methods can search both local optimal solutions and the global one depending on the problem domain and time limit.

Due to the population-based search capability as well as simplicity, convergence speed, and robustness, PSO-based optimization algorithms, are widely used for handling multi-objective optimization problems, although the performance of a conventional PSO algorithm greatly depends on its parameter and it may face the danger of being trapped in local optima [36–41]. To handle these issues suitably and improve the performance of a conventional PSO algorithm, an expert AMPSO (Adaptive Modified Particle Swarm Optimization) algorithm is proposed in this paper and implemented to solve the multi-operation management problem inside a typical MG for a time period of 24 h considering economy and emission as competitive objectives. It's noteworthy that from an optimal operation planning point of view, a grid operation can be optimized globally or locally. When a global optimization is adopted, conventional OPF (Optimal Power Flow) methods are widely used because they consider different aspects of a grid topology together with all controllable variables such as transformers taps, capacitors, feeder reconfigurations and etc. Besides,

such methods are usually run for the time horizon of 1 h considering various objectives such as minimum fuel cost, emission, transmission loss, switching and time simultaneously. Since in this paper the optimal operation of a MG is selected as the benchmark which is a local optimization problem and lacks several features of global one mentioned earlier, the conventional OPF is no longer used. Moreover, because the objectives are not the same, instead of a single solution, a pareto front of optimal solutions will be obtained for the mentioned problem which are stored in a finite-sized repository. A Fuzzy clustering approach is also used to control the size of repository up to a limit range. To overcome the local optima problem from one side and to improve the approach performance from the other side a hybrid approach including a FSA (Fuzzy Self Adaptive) mechanism and a CLS (Chaotic Local Search) method is adopted. A prominent feature of the proposed approach is that it provides a true and well-distributed set of non-dominated pareto-optimal solutions with fast convergence and low computational time. The feasibility of the proposed method is also tested in a MG with five DG units.

The rest of the paper is organized as follows: Section 2 formulates the multi-objective optimization problem together with its related equality and inequality constraints. A brief description of the test MG is presented in Section 3. Fundamentals of multi-objective optimization are covered in Section 4. A fuzzy-based clustering approach to control the size of repository is presented in Section 5. The proposed AMPSO algorithm is discussed in Section 6. Section 7 deals with the implementation of the proposed AMPSO algorithm to the multi-operation management of the test system. Finally, in Section 8, the great performance of the proposed method and its feasibility is demonstrated and compared to those of other evolutionary-based optimization approaches.

2. Problem formulation

The multi-operation management problem in a typical MG is defined as a problem to allocate optimal power generation set points as well as suitable ON or OFF states to DG units in a sense that the operating cost of the MG and the net pollutants emission inside the grid are minimized simultaneously while satisfying several equality and inequality constraints. The mathematical model of such problem can be expressed as follows.

2.1. Objective functions

2.1.1. Objective 1: Operating Cost Minimization

The total operating cost of the MG in €ct (Euro cent) includes the fuel costs of DGs, start-up/shut-down costs and the costs of power exchange between the MG and the utility. The cost objective function aims at finding OPFs from energy sources to load centers for a definite period of time in an economical manner. Such objective function can be formulated as below:

$$\begin{aligned}\text{Min } f_1(X) &= \sum_{t=1}^{T}\text{Cost}^t = \sum_{t=1}^{T}\left\{\sum_{i=1}^{N_g}[u_i(t)P_{Gi}(t)B_{Gi}(t)+S_{Gi}|u_i(t)\right.\\ &\quad -u_i(t-1)|]+\sum_{j=1}^{N_s}\left[u_j(t)P_{sj}(t)B_{sj}(t)+S_{sj}|u_j(t)-u_j\right.\\ &\quad \left.\left.(t-1)|\right]+P_{\text{Grid}}(t)B_{\text{Grid}}(t)\right\} \qquad (1)\end{aligned}$$

where $B_{Gi}(t)$ and $B_{Sj}(t)$ are the bids of the DGs and storage devices at hour t, S_{Gi} and S_{sj} represent the start-up or shut-down costs for ith DG and jth storage respectively, $P_{\text{Grid}}(t)$ is the active power which is bought (sold) from (to) the utility at time t and $B_{\text{Grid}}(t)$ is the bid of utility at time t. X is the state variables vector which includes active power of units and their related states and is described as follows:

$$\begin{aligned}X &= [P_g, U_g]_{1\times 2nT}\\ P_g &= [P_G, P_s]\\ n &= N_g + N_s + 1\end{aligned} \qquad (2)$$

where, n is number of state variables, N_g and N_s are the total number of generation and storage units respectively, P_g is the power vector including active powers of all DGs and U_g is the state vector denoting the ON or OFF states of all units during each hour of the day. These variables can be described as follows:

$$\begin{aligned}&P_G = \left[P_{G1}, P_{G2}, \ldots, P_{G,N_g}\right]\\ &P_{Gi} = [P_{Gi}(1), P_{Gi}(2), \ldots, P_{Gi}(t), \ldots, P_{Gi}(T)];\ i = 1,2,\ldots,N_g+1\\ &P_s = \left[P_{s1}, P_{s2}, \ldots, P_{s,N_s}\right]\\ &P_{sj} = \left[P_{sj}(1), P_{sj}(2), \ldots, P_{sj}(t), \ldots, P_{sj}(T)\right];\ j = 1,2,\ldots,N_s\end{aligned} \qquad (3)$$

where T represents total number of hours, $P_{Gi}(t)$ and $P_{sj}(t)$ are the real power outputs of ith generator and jth storage at time t respectively.

$$\begin{aligned}&U_g = [u_1, u_2, \ldots, u_n] = \{u_i\}_{1\times n} \in \{0,1\};\\ &u_k = [u_k(1), u_k(2), \ldots, u_k(t), \ldots, u_k(T)];\quad k = 1,2,\ldots,n\end{aligned} \qquad (4)$$

where $u_k(t)$ is the status of unit k at hour t.

2.1.2. Objective 2: Pollutants emission minimization

In the next step, the environmental footprints from atmospheric pollutants are considered as the second objective. In this regard, three of the most important pollutants are involved in the objective function: CO_2 (carbon dioxide), SO_2 (sulfur dioxide) and NO_x (nitrogen oxides). The mathematical formulation of the second objective can be described as follow:

$$\begin{aligned}\text{Min } f_2(X) &= \sum_{t=1}^{T}\text{Emission}^t = \sum_{t=1}^{T}\left\{\sum_{i=1}^{N_g}[u_i(t)P_{Gi}(t)E_{Gi}(t)]\right.\\ &\quad \left.+\sum_{j=1}^{N_s}\left[u_j(t)P_{sj}(t)E_{sj}(t)\right]+P_{\text{Grid}}(t)E_{\text{Grid}}(t)\right\}\end{aligned} \qquad (5)$$

where all the above parameters are defined as before, $E_{Gi}(t)$, $E_{sj}(t)$ and $E_{\text{Grid}}(t)$ are described as the amount of pollutants emission in kg MW h^{-1} for each generator, storage device and utility at hour t respectively. These emission variables are as follow:

$$E_{Gi}(t) = \text{CO}_{2_{\text{DG}_i}} + \text{SO}_{2_{\text{DG}_i}}(t) + \text{NO}_{x_{\text{DG}_i}}(t) \qquad (6)$$

where $\text{CO}_{2_{DG_i}}(t), \text{SO}_{2_{DG_i}}(t)$ and $\text{NO}_{x_{DG_i}}(t)$ are the amounts of CO_2, SO_2 and NO_x emission from ith DG sources at hour t respectively.

$$E_{sj}(t) = \text{CO}_{2_{\text{Storage}_j}}(t) + \text{SO}_{2_{\text{Storage}_j}}(t) + \text{NO}_{x_{\text{Storage}_j}}(t) \qquad (7)$$

where $\text{CO}_{2_{\text{Storage}_j}}(t), \text{SO}_{2_{\text{Storage}_j}}(t)$ and $\text{NO}_{x_{\text{Storage}_j}}(t)$ are the amounts of CO_2, SO_2 and NO_x emission from jth storage unit during tth hours of the day respectively.

$$E_{\text{Grid}}(t) = \text{CO}_{2_{\text{Grid}}}(t) + \text{SO}_{2_{\text{Grid}}}(t) + \text{NO}_{x_{\text{Grid}}}(t) \qquad (8)$$

where $CO_{2_{Grid}}(t), SO_{2_{Grid}}(t)$ and $NO_{x_{Grid}}(t)$ are the amounts of CO_2, SO_2 and NO_x emission from utility or macro-grid at hour t respectively.

2.2. Constraints

2.2.1. Power balance

The total power generation from DGs in the MG must cover the total demand inside the grid. Since a small 3-feeder radial L.V system is proposed in the work, there is no urgent need to consider transmission losses which are low numerically. Hence,

$$\sum_{i=1}^{N_g} P_{Gi}(t) + \sum_{j=1}^{N_s} P_{sj}(t) + P_{\mathrm{Grid}}(t) = \sum_{k=1}^{N_k} P_{Lk}(t) \tag{9}$$

where P_{Lk} is the amount of kth load level and N_k is the total number of load levels.

2.2.2. Real power generation capacity

For a stable operation, the active power output of each DG is limited by lower and upper bounds as follows:

$$\begin{aligned} &P_{Gi,\min}(t) \le P_{Gi}(t) \le P_{Gi,\max}(t) \\ &P_{sj,\min}(t) \le P_{sj}(t) \le P_{sj,\max}(t) \\ &P_{\mathrm{grid},\min}(t) \le P_{\mathrm{Grid}}(t) \le P_{\mathrm{grid},\max}(t) \end{aligned} \tag{10}$$

where $P_{G,\min}(t)$, $P_{s,\min}(t)$ and $P_{\mathrm{grid},\min}(t)$ are the minimum active powers of ith DG, jth storage and the utility at the time t. In a similar manner, $P_{G,\max}(t)$, $P_{s,\max}(t)$ and $P_{\mathrm{grid},\max}(t)$ are the maximum power generations of corresponding units at hour t.

2.2.3. Battery limits

Since there are some limitations on charge and discharge rate of storage devices during each time interval, the following equation and constraints can be expressed for a typical battery:

$$W_{\mathrm{ess},t} = W_{\mathrm{ess},t-1} + \eta_{\mathrm{charge}} P_{\mathrm{charge}} \Delta t - \frac{1}{\eta_{\mathrm{discharge}}} P_{\mathrm{discharge}} \Delta t \tag{11}$$

$$\begin{cases} W_{\mathrm{ess},\min} \le W_{\mathrm{ess},t} \le W_{\mathrm{ess},\max} \\ P_{\mathrm{charge},t} \le P_{\mathrm{charge},\max}; \quad P_{\mathrm{discharge},t} \le P_{\mathrm{discharge},\max} \end{cases} \tag{12}$$

where $W_{\mathrm{ess},t}$ and $W_{\mathrm{ess},t-1}$ are the amount of energy storage inside the battery at hour t and $t-1$ respectively, $P_{\mathrm{charge}}(P_{\mathrm{discharge}})$ is the permitted rate of charge(discharge) during a definite period of time (Δt), $\eta_{\mathrm{charge}}(\eta_{\mathrm{discharge}})$ is the efficiency of the battery during charge(discharge) process. $W_{\mathrm{ess},\min}$ and $W_{\mathrm{ess},\max}$ are the lower and upper limits on amount of energy storage inside the battery and $P_{\mathrm{charge},\max}(P_{\mathrm{discharge},\max})$ is the maximum rate of battery charge(discharge) during each time interval Δt.

3. MG modeling

MG, in its whole vision, is an exemplar of a macro-grid in which local energy potentials are mutually connected with each other as well as with the L.V utility and make a small-scaled power grid. In such a network, DGs are exploited extensively both in forms of renewable (e.g., wind and solar) and non-conventional (MT (micro-turbine), fuel cell, diesel generator) resources because these emerging prime movers have lower emission and the potential to have lower cost negating traditional economies of scale [42]. In addition to DGs, storage options are also used widely to offset expensive energy purchases from utility or to store energy during off-peak hours for an anticipated price spike. In a typical MG, DERs generally have different owners handle the autonomous operation of the grid with the help of Local Controllers (μ_c or MGLC) which are joined with each DER and μ_{cc} or MGCC (Micro-Grid Central Controller). Moreover, the CCU (Central Control Unit), which is a part of the MGCC, does the optimization process to achieve a robust and optimal plan of action for the smart operation of the MG. The raw input data to this unit includes the amount of load inside the grid and the powers generated by the nonscheduled DGs typically based on RESs (Renewable Energy Sources) and the output information involves the optimal set points for DGs in terms of suitable ON/OFF states and required active and reactive powers for supplying the load while keeping the node voltages within the range specified by Norm EN 50160 [43].

In this paper, a typical L.V MG is considered as the test system for application of suggested methodology. The proposed MG includes various DG sources such as MT, a low temperature PAFC (Phosphoric Acid Fuel Cell), PV, WT (Wind Turbine) and a NiMH-Battery (Nickel-Metal-Hydride battery) as shown in Fig. 1. The back-up MT/PAFC/NiMH-Battery hybrid power source is situated at different locations in the MG, to level the mismatch between renewable power generators and consumption and/or to store the surplus of power from renewable sources for later use during non-generation or low power generation time periods. It is assumed that all DGs produce active power at unity power factor, neither requesting nor producing reactive power. Besides, all units in this paper are assumed to be operating in electricity mode only and no heat is required for the examined period. There is also an electrical link for power exchange between the MG and the utility during different hours of a day based on decisions made by MGCC.

4. Fundamentals of multi-objective optimization

Multi-objective optimization is a concept associated with many real-world optimization problems which aim at finding optimal solutions considering different objectives simultaneously. These multi-criteria optimization problems can not be handled through finding a single optimal solution, because a particular solution isn't the best with regard to all objectives. Therefore, a multi-objective optimization problem leads to a set of optimal solutions known as Pareto-optimal. Generally, in a multi-objective optimization problem there are different objective functions required to be optimized simultaneously considering a set of equality and inequality constraints as follows [44,45]:

$$\begin{aligned} &\text{Minimize } F = [f_1(X), f_2(X), \ldots, f_n(X)]^T \\ &\text{Subject to}: \begin{cases} g_i(X) < 0 & i = 1, 2 \ldots, N_{ueq} \\ h_i(X) = 0 & i = 1, 2 \ldots, N_{eq} \end{cases} \end{aligned} \tag{13}$$

where, F is a vector including objective functions and X is a vector containing optimization variables, $f_i(X)$ is the ith objective function, $g_i(X)$ and $h_i(X)$ are the equality and inequality constraints respectively and n is the number of objective functions. For a multi-objective optimization problem, any two solutions X and Y can have one of these two possibilities: one dominates the other or none dominates the other. In a minimization problem, without loss of generality, a solution X dominates Y if the following two conditions are satisfied:

$$\begin{aligned} &\forall j \in \{1, 2, \ldots, n\}, \ f_j(X) \le f_j(Y) \\ &\exists k \in \{1, 2, \ldots, n\}, \ f_k(X) < f_k(Y) \end{aligned} \tag{14}$$

Through the entire search space, the non-dominated solutions are considered as "*Pareto-optimal*" and form the *Pareto-optimal set* or *Pareto-optimal front*. Likewise, "*Pareto-dominance*" is a concept used for determining the eligibility of each particle (or solution) to be stored in the repository of non-dominated solutions. A feasible

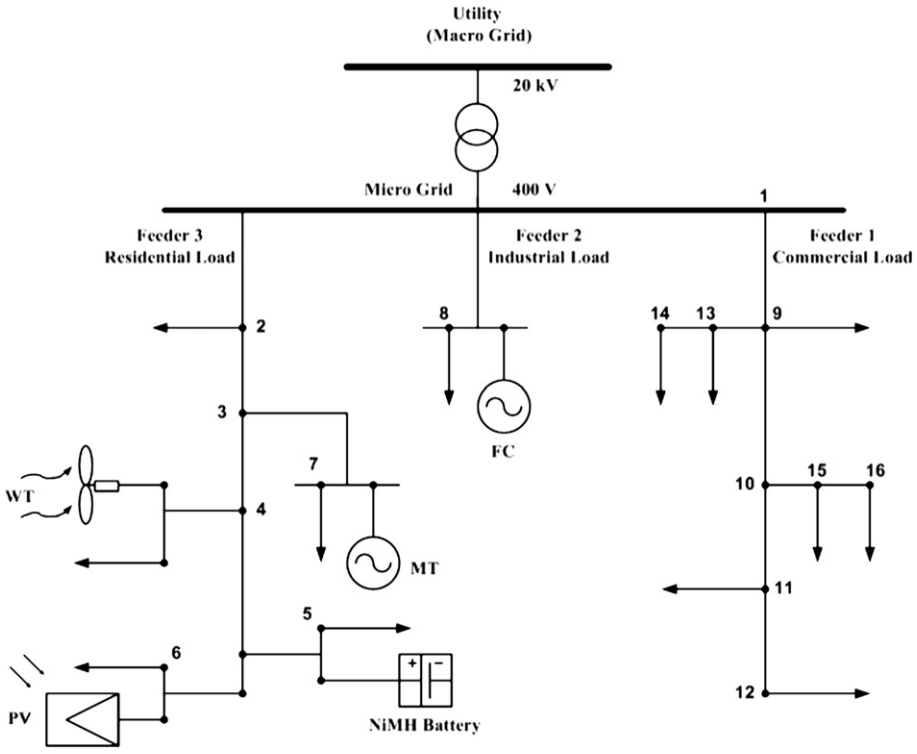

Fig. 1. A typical L.V micro-grid.

solution can be added to the repository if it satisfies any of the following conditions [46]:

- The repository is full but the candidate solution is non-dominated and it is in a less crowded region than at least one solution,
- The repository is not full and the candidate solution is not dominated by any solution in the repository,
- The candidate solution dominates all the solutions in the repository,
- The repository is empty.

5. Fuzzy clustering for control the size of repository

It was mentioned earlier that in a multi-objective optimization problem, non-dominated solutions are stored in a predefined repository. Since the repository of non-dominated solutions has a finite size, a limited number of candidate solutions can be stored and the rest should be omitted. Up to now, various techniques based on artificial intelligence have been proposed for controlling the size of repository [47] and in this paper, a fuzzy-based clustering approach has been applied to do the same task. First, a fuzzy membership function is used to evaluate each objective function related to any individual inside the repository as follows:

$$\mu_{f_i}(X) = \begin{cases} 1, & f_i(X) \le f_i^{\min} \\ 0, & f_i(X) \ge f_i^{\max} \\ \dfrac{f_i^{\max} - f_i(X)}{f_i^{\max} - f_i^{\min}}, & f_i^{\min} \le f_i(X) \le f_i^{\max} \end{cases} \tag{15}$$

where $f_i^{\min}$ and $f_i^{\max}$ are the lower and upper bounds of ith objective function, respectively. In the proposed algorithm, the values of $f_i^{\min}$ and $f_i^{\max}$ are evaluated by optimizing each objective function separately. In the next step, the normalized membership value is calculated for each element inside the repository, as follows:

$$N\mu(j) = \frac{\sum_{k=1}^{n} \omega_k \times \mu_{fk}(X_j)}{\sum_{j=1}^{m} \sum_{k=1}^{n} \omega_k \times \mu_{fk}(X_j)} \tag{16}$$

where m is the number of non-dominated solutions, ω_k is the weight factor for kth objective function. The normalized

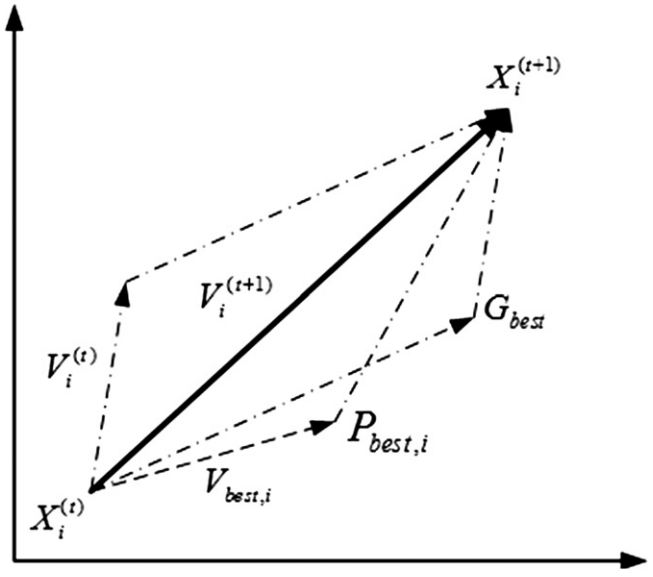

Fig. 2. Fundamental elements for a particle displacement in PSO algorithm.

membership value is a decisive criterion used for storing the best non-dominated solutions in the repository i.e., in a fuzzy clustering approach for control the size of repository, initially the normalized membership values are calculated and sorted, then, the best individuals are selected and stored in the repository.

6. PSO algorithm

Among the evolutionary-based optimization algorithms, PSO has been significantly used in multi-objective problems mainly due to its population-based search capability as well as simplicity, convergence speed, and robustness. It was first introduced by Kennedy and Eberhart [48] and was based on the imitation of animals' social behaviors using tools and ideas taken from computer graphics and social psychology research. Usually, PSO simulates the behaviors of a flock of bird called "*swarm*" in which any single and feasible solution is a bird and is called "*particle*". Each particle has its own fitness value evaluated by the fitness function, and has a velocity vector which addresses the flying of the particle. To reach the optimal point, particles must update their next displacements according to their own velocities, their best performances and the best performance of their best informant as shown in Fig. 2 and formulated as follows:

$$V_i^{(k+1)} = \omega \times V_i^{(k)} + C_1 \times \mathrm{rand}_1(\cdot) \times \left(P_{\mathrm{best},i} - X_i^{(k)}\right) + C_2 \times \mathrm{rand}_2(\cdot) \times \left(G_{\mathrm{best}} - X_i^{(k)}\right) \quad (17)$$

$$X_i^{(k+1)} = X_i^{(k)} + V_i^{(k+1)} \quad (18)$$

where $V_i^{(k+1)}$ is the updated velocity vector of ith particle based on the three displacement fundamentals, $X_i^{(k+1)}$ is the updated position of ith particle, $\mathrm{rand}_1(\cdot)$ and $\mathrm{rand}_2(\cdot)$ denote two random numbers in the range [0,1] , C_1 and C_2 are the learning factors and ω refers to inertia or momentum weight factor. $P_{\mathrm{best},i}$ is the best previous experience of ith particle that is recorded and G_{best} is the best particle (informant) among the entire population.

6.1. Binary PSO

To extend the real-valued PSO to discrete space where it is needed, Kennedy and Eberhart calculate probability from the velocity to determine whether $X_i^{(k+1)}$ will be in ON state or OFF (0/1). They squashed $V_i^{(k+1)}$ using the following logistic functions [49]:

$$\rho\left(V_i^{(k+1)}\right) = \frac{1}{1+\exp\left(-V_i^{(k+1)}\right)} \quad (19)$$

$$X_i^{(k+1)} = \begin{cases} 1, & \text{if } \mathrm{rand}(\cdot) < \rho\left(V_i^{(k+1)}\right) \\ 0, & \text{otherwise} \end{cases} \quad (20)$$

where $\mathrm{rand}(\cdot)$ is a uniform distribution in [0,1].

6.2. The proposed AMPSO approach

It was observed in the previous section that the performance of a classic PSO algorithm depends greatly on three influential parameters usually stated as the exploration–exploitation trade-off: learning factors (C_1, C_2) and momentum weight factor (ω). Since a standard PSO algorithm along with a given set of parameters is not capable of dealing with multi-objective optimization problems appropriately in all situations, some modifications are become necessary. In this paper, an adaptive modified PSO algorithm is proposed in order to improve the performance of a standard PSO approach and facilitate the multi-objective optimization process.

6.2.1. CLS mechanism

To enrich the search behavior and avoid the premature phenomenon of PSO in solving multi-operation management problem, incorporating a chaotic search into PSO to construct a CPSO (chaotic PSO) is proposed. The chaotic search algorithm is developed from the chaotic evolution of variables. Two well-known chaotic maps, logistic map and tent map, are the most common maps used in chaotic searches [50,51]. A rough description of chaos is that chaotic systems exhibit a great sensitivity to initial conditions. Due to the unique ergodicity characteristic, inherent stochastic property and irregularity of chaos, a chaotic can traverse every state in a certain space by its own regularity and visit every state once only, which helps avoid being trapped in local optima. Thus, a chaotic search has a much higher precision than some other stochastic algorithms.

6.2.1.1. CLS type-1. The first CLS mechanism is an approach which is based on the logistic map. The feature of the logistic map is that a small difference in the initial value of the chaotic variable would result in a considerable difference in its long-time behaviors. The relative simplicity of the logistic map makes it an excellent point of entry into a consideration of the concept of chaos. Generally a logistic map is considered as follow:

$$\begin{aligned} Cx_i &= \left[cx_i^1, cx_i^2, \ldots, cx_i^n\right]_{1\times n}, \quad i = 0,1,2,\ldots,N_{\mathrm{chaos}} \\ cx_{i+1}^j &= 4 \times cx_i^j \times \left(1 - cx_i^j\right), \quad j = 1,2,\ldots,n \\ cx_i^j &\in [0,1], \quad cx_0^j \notin \{0.25, 0.5, 0.75\} \\ cx_0^j &= \mathrm{rand}(\cdot) \end{aligned} \quad (21)$$

where, cx_i^jindicates the jth chaotic variable, N_{chaos} is the number of individuals for CLS, n is the number of DGs and rand(·) is a random number between 0 and 1. In this approach, first a particle is selected randomly from the repository (X_g) and considered as an initial population for CLS (X_{cls}^0). At the second step the initial population is scaled into [0,1] as follows:

$$\begin{aligned} X_{\mathrm{cls}}^0 &= \left[x_{\mathrm{cls},0}^1, x_{\mathrm{cls},0}^2, \ldots, x_{\mathrm{cls},0}^n\right]_{1\times n} \\ Cx_0 &= \left[cx_0^1, cx_0^2, \ldots, cx_0^n\right] \\ cx_0^j &= \frac{x_{\mathrm{cls},0}^j - P_{\mathrm{min,unit}}^j}{P_{\mathrm{max,unit}}^j - P_{\mathrm{min,unit}}^j}, \quad j = 1,2,\ldots,n \end{aligned} \quad (22)$$

where $P_{\mathrm{min,unit}}^j$ and $P_{\mathrm{max,unit}}^j$ are the lower and upper limits of active power for jth generation unit. The chaos population for CLS is generated as follows:

$$\begin{aligned} X_{\mathrm{cls}}^i &= \left[x_{\mathrm{cls},i}^1, x_{\mathrm{cls},i}^2, \ldots, x_{\mathrm{cls},i}^n\right]_{1\times n} \qquad i = 1,2,\ldots,N_{\mathrm{choas}} \\ x_{\mathrm{cls},i}^j &= cx_{i-1}^j \times \left(P_{\mathrm{max,unit}}^j - P_{\mathrm{min,unit}}^j\right) + P_{\mathrm{min,unit}}^j, \quad j = 1,2,\ldots,n \end{aligned} \quad (23)$$

In the next step, the objective functions are calculated for any member of the population and the non-dominated solutions are found and sorted into a separate memory subsequently. The way in which one non-dominated solution is replaced with a particle selected randomly from the swarm is shown in Fig. 3.

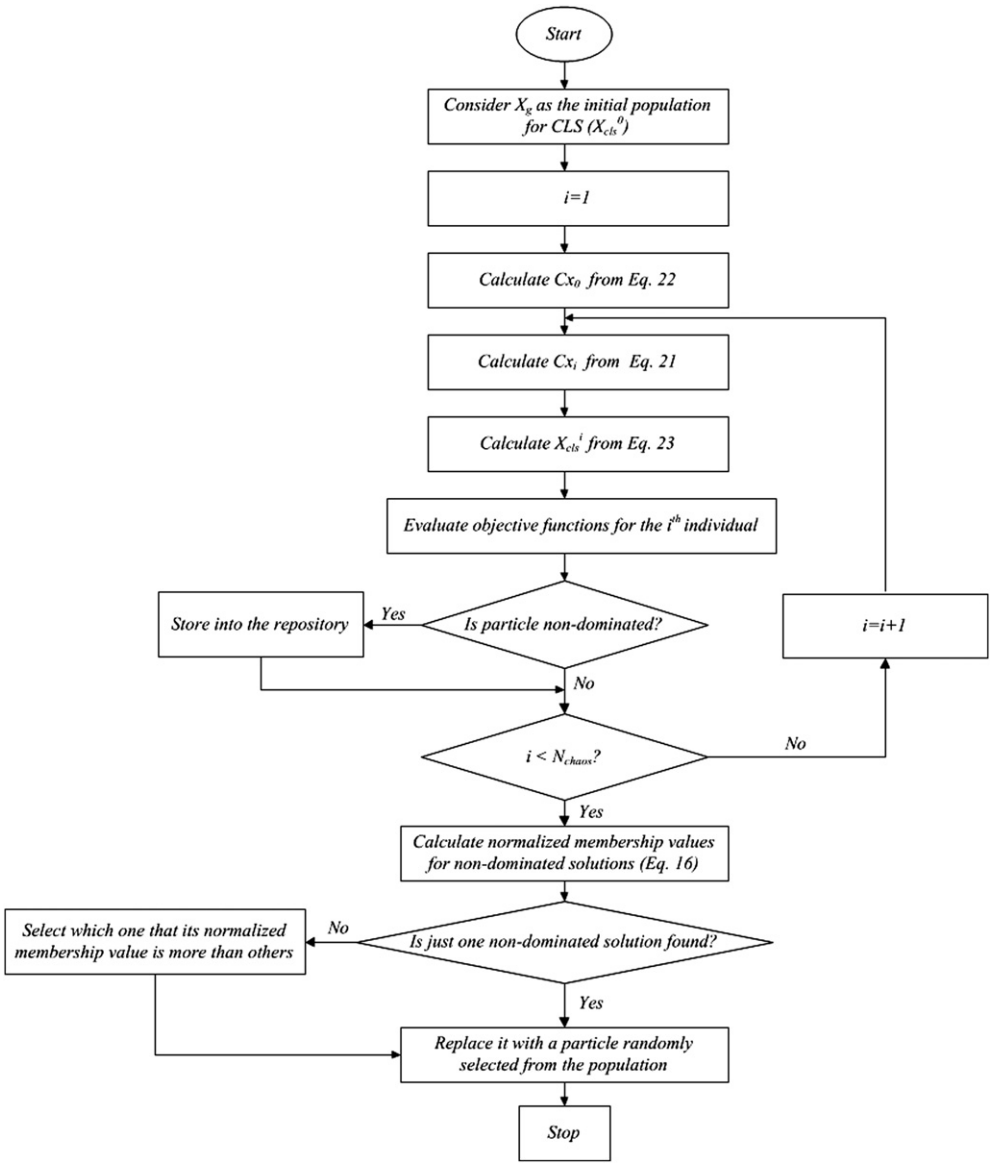

Fig. 3. Chaotic Local Search (CLS) flowchart.

6.2.1.2. CLS type-2. The CLS type-2 is a procedure similar to the first one but is based on the tent equation. In this mechanism the chaotic variables are defined as follows while the other instructions remain unchanged.

$$Cx_i = \left[cx_i^1, cx_i^2, \ldots, cx_i^n\right]_{1\times n} \qquad i = 0,1,2,\ldots,N_{\text{chaos}}$$
$$cx_{i+1}^j = \begin{cases} 2cx_i^j, & 0 < cx_i^j \le 0.5 \\ 2\left(1-cx_i^j\right), & 0.5 < cx_i^j \le 1 \end{cases} \quad j = 1,2,\ldots,n \qquad (24)$$
$$cx_0^j = \text{rand}(\cdot)$$

6.2.2. FSA mechanism

In a classic PSO approach the momentum weight factor (ω) is widely used both for controlling the scope of the search and reducing the importance of maximum velocity while the learning factors (C_1 and C_2) are used for finding the optimum point through concentration on promising candidate solutions. In this regard, C_1 has a contribution toward self-exploration of a particle while C_2 has a contribution toward motion of the particles in global direction considering the motion of all the particles in the preceding program iterations.

To overcome all the deficiencies associated with a conventional PSO algorithm, a FSAPSO (Fuzzy Self Adaptive PSO) mechanism is developed to adjust the inertia weight and the learning factors when they are needed. For this purpose, two triangular membership functions are proposed; one for the learning factors adjustment and the other for weight inertia tuning, as shown in Figs. 4 and 5. The input set for learning factors adjustment are the best fitness (BF) and the number of generations for unchanged best fitness (NU) while the best fitness (BF) and the inertia weight (ω) are the input set for the second membership function. In the first membership function linguistic variables for inputs (NBF, NU) and outputs (C_1, C_2) are as following: Positive Small (PS), Positive Medium (PM), Positive Big (PB) and Positive Bigger (PR). Similarly, for the second membership function linguistic values

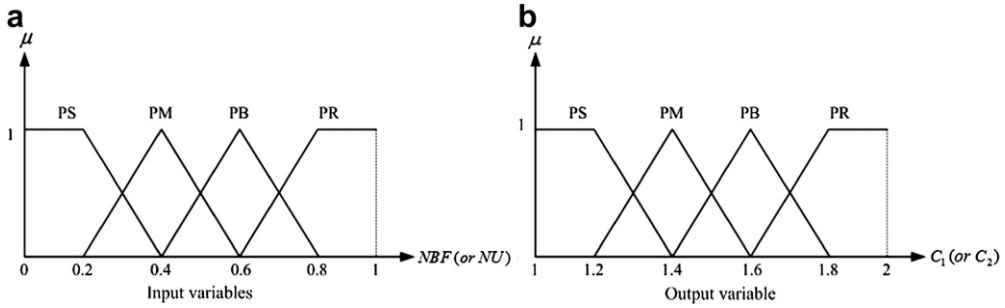

Fig. 4. Membership functions of input/output variables for learning factors.

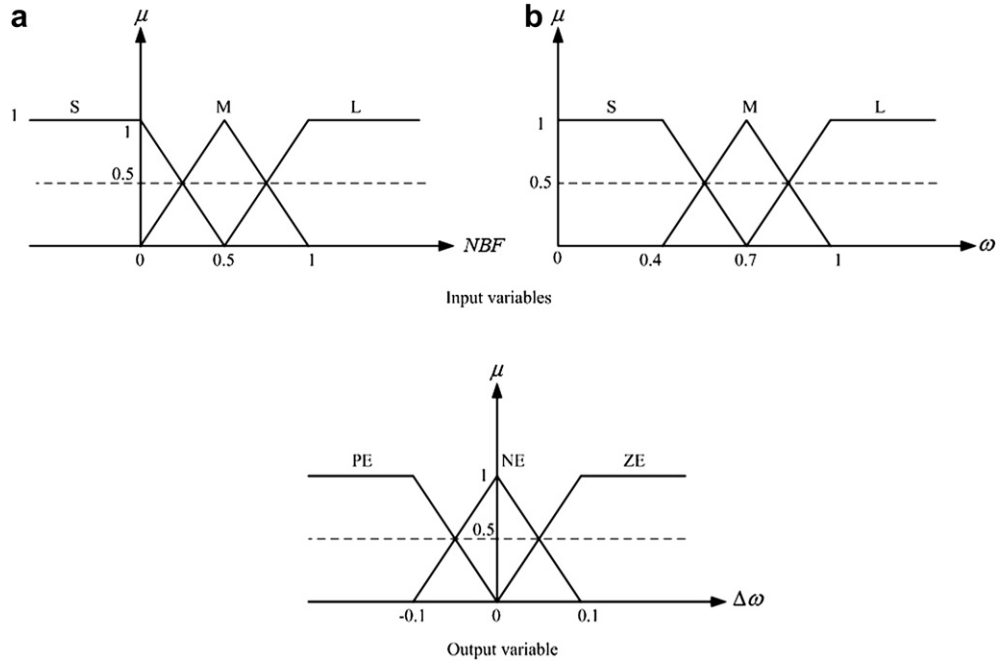

Fig. 5. Membership functions of input/output variables for inertia weight correction factor.

can be defined as follows: Small (S), Medium (M) and Large (L) for the input set (NBF, ω) and Negative (NE), Zero (ZE) and Positive (PE) for the output variable ($\Delta\omega$). Since either a positive or negative value may be assigned to $\Delta\omega$ therefore, a range of $(-1, +1)$ has been preferred for the inertia weight correction as stated in Eq. (25).

$$\omega^{k+1} = \omega^{k} + \Delta\omega \tag{25}$$

Furthermore, to make a robust approach, BF and NU values can be normalized into [0,1] as shown in Eq. (26)

$$\mathrm{NBF} = (\mathrm{BF} - \mathrm{BF}_{\min})/(\mathrm{BF}_{\max} - \mathrm{BF}_{\min}) \tag{26}$$

where $\mathrm{BF}_{\min}$ is the minimum fitness value and $\mathrm{BF}_{\max}$ is the fitness value which is greater or equal to the maximum fitness value. Additionally, values of ω, C_1 and C_2 are limited as follows:

$$\begin{aligned} &0.4 \le \omega \le 1 \\ &1 \le C_1 \le 2; \quad 1 \le C_2 \le 2 \end{aligned} \tag{27}$$

To express the conditional statements which represent a mapping from the input space to output space the Mamdani fuzzy rule is adopted and the corresponding conditions are tabulated in Tables 1–3. As examples of conditional statements the following fuzzy rules can be considered:

If (NBF is PB) & (NU is PM), *Then* (C_1 is PM)
or:
If (NBF is *L*) & (ω is *S*), *Then* ($\Delta\omega$ is NE)

7. AMPSO implementation

To apply the proposed AMPSO algorithm in multi-operation management and optimal power dispatch problem a hierarchical structure and a top-down procedure must be followed as stated below:

Table 1
Fuzzy rules for learning factor C_1.

C_1		NU			
		PS	PM	PB	PR
NBF	PS	PR	PB	PB	PM
	PM	PB	PM	PM	PS
	PB	PB	PM	PS	PS
	PR	PM	PM	PS	PS

Table 2
Fuzzy rules for learning factor C_2.

C_2		NU			
		PS	PM	PB	PR
NBF	PS	PR	PB	PM	PM
	PM	PB	PM	PS	PS
	PB	PM	PM	PS	PS
	PR	PM	PS	PS	PS

Step 1: Input data definition

At the beginning of the program required input data must be provided precisely. This information includes: MG configuration, operational characteristics of DGs and the utility, predicted output powers of WT and PV for a day ahead, hourly bids of DGs and the utility, emission coefficients of mentioned units, objective functions and the MG daily load curve.

Step 2: Program initialization

At the second step the program must be initialized by a set of random populations and their corresponding velocities as follows:

$$\begin{aligned}&\text{Population} = \left[X_1 \;\; X_2 \;\; \cdots \;\; X_{N_{\text{swarm}}}\right]^T\\ &X_0 = \left[x_0^1, x_0^2, \ldots, x_0^n\right]\\ &x_0^j = \text{rand}(\cdot)\times\left(x_j^{\max} - x_j^{\min}\right) + x_j^{\min};\;\; X_i = \left[x_i^j\right]_{1\times n}\\ &j = 1,2,3,\ldots,n;\;\; i = 1,2,\ldots,N_{\text{swarm}};\;\; n = 2\times\left(N_g + N_s + 1\right)\end{aligned} \tag{28}$$

$$\begin{aligned}&\text{Velocity} = \left[V_1 \;\; V_2 \;\; \cdots \;\; V_{N_{\text{swarm}}}\right]^T\\ &V_i = \left[v_i\right]_{1\times n}\\ &v_i = \text{rand}(\cdot)\times\left(v_i^{\max} - v_i^{\min}\right) + v_i^{\min};\\ &i = 1,2,3,\ldots,N_{\text{swarm}};\quad n = 2\times\left(N_g + N_s + 1\right)\end{aligned} \tag{29}$$

where, n is the number of state variables, vi and xi are the velocity and position of the ith state variable respectively. rand(·) is a random number between 0 and 1.

Step 3: do ($i = 1$)

Step 4: Select the ith individual and calculate the values of corresponding objective functions

For the selected individual, the values of objective functions are calculated separately using the dispatch algorithm illustrated in Fig. 6.

Step 5: Store the ith individual in the repository if it is a non-dominated solution and apply the fuzzy clustering approach for controlling the size of repository.

Step 6: Find the local best solution for ith individual ($P_{\text{best},i}$)

At the beginning of the program, the initial generated populations are considered as local best solutions. During any iteration of the program if one of the following criteria is satisfied then the local best solutions are updated, otherwise they remain unchanged:

(i) If the former local best is dominated by the current one, then the later is selected as the local best solution,

(ii) If none of them dominates each other, the one with the higher normalized membership function is considered as the local best.

Table 3
Fuzzy rules for inertia weight correction factor.

$\Delta\omega$		ω		
		S	M	L
NBF	S	ZE	NE	NE
	M	PE	ZE	NE
	L	PE	ZE	NE

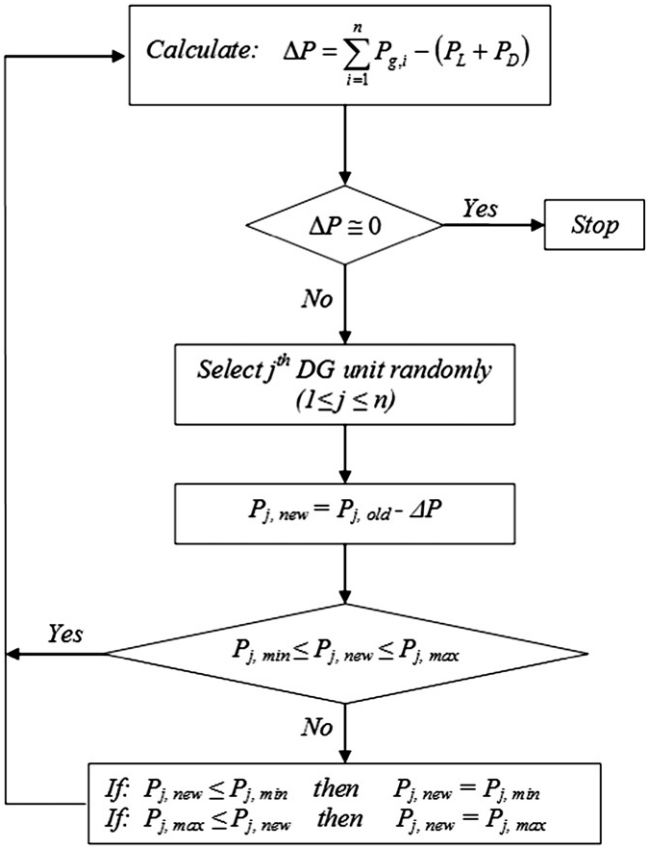

Fig. 6. Flowchart of power dispatch algorithm.

Step 7: $i = i + 1$

Step 8: While ($i \le N_{\text{swarm}}$) redo steps 4–7

Step 9: Select the global best (G_{best})

In this step, the global best solution is selected randomly from the candidate solutions. To define G_{best} value, first the normalized membership values must be calculated for all of the non-dominated solutions inside the repository using Eq. (16)

$$N\mu = \left[N\mu_1, N\mu_2, \ldots, N\mu_i, \ldots, N\mu_m\right]_{1\times k} \tag{30}$$

where, Nμi is the normalized membership value for the ith non-dominated solution and k is the size of repository. Afterward, the cumulative probabilities of the individuals are calculated as follows:

$$\begin{aligned}&C_i = \left[C_1, C_2, \ldots, C_m\right]_{1\times k}\\ &\begin{cases} C_1 = N\mu_1\\ C_2 = C_1 + N\mu_2\\ \vdots\\ C_k = C_{k-1} + N\mu_k\end{cases}\end{aligned} \tag{31}$$

where, Ci is the cumulative probability for the ith individual. Finally, the best global position inside the search space is selected randomly using the roulette wheel approach. In this regard, a random number between 0 and 1 is generated and compared with the values of calculated cumulative probabilities. The first cumulative probability term which is greater than the generated number, is the target value and the associated position is considered as the best global position.

Step 10: Update the population and find new solutions.
The whole population is updated using the AMPSO algorithm. In this step all of the PSO parameters such as learning factors and inertia weight are adjusted by the FSA approach while the search ability is improved by the CLS mechanism.

Step 11: Check the termination criteria.
If the maximum number of iterations executed by the AMPSO is met or the desired error is reached, the optimization procedures are stopped, otherwise the population is replaced with the new generation and the algorithm is repeated from step 3.

8. Simulation results

In this part of the work the proposed AMPSO algorithm is implemented to solve the multi-operation management problem for a typical MG as shown in Fig. 1. Since the two conflicting objectives (cost and emission) must be taken into account and minimized simultaneously, a set of optimal solutions known as *Pareto-optimal* will be obtained for the mentioned problem. Regarding a Pareto-optimal set, there is a strong need to find the extreme points of the trade-off front and this can be easily done by solving the operation management problem with respect to each objective function separately. Moreover, to get better insight to the extreme points, the problem is solved in three different cases including the main case, where all the units are dispatched regarding their real constraints, the second case in which both RESs (WT and PV) act at their maximum output powers (*Max-Renw*) and the third case in which the utility can exchange energy with the MG infinitely (*Inf-Eneg.Exch*). The main reason for selecting such cases is originated from the background knowledge of authors from power market planning and practical considerations in DG management. For the entire cases, the load demand within the MG for a typical day comprises one primarily residential area, one industrial feeder serving a small workshop and one feeder with light commercial consumers which is equivalent to a total energy demand of 1695 kwh for the mentioned day as shown in Fig. 7. The real-time market energy prices for the examined period of time are considered as Table 4. For allocation of optimal set points to the units through the entire case studies, all DGs are considered to be "ON" or in state "1", thus there will be no start-up or shut-down cost for the mentioned units. The minimum and maximum power generation limits of the DGs are given in Table 5. The bid coefficients in cents of Euro (€ct) per kilo-Watt hour (kWh) as well as emissions in kilogram per MWh for DGs are given in Table 6. In the same table, start-up/shut-down costs where applicable are presented. To simplify our analysis, all units in this paper are assumed to be operating in electricity mode only and no heat is required for the examined period. The maximum power outputs obtained from RESs are also estimated for a day ahead using an expert prediction model and neural networks which is out of the scope of this paper and will be presented in future works. Such predicted values are shown in Fig. 8 and tabulated in Table 7 for WT and PV correspondingly. Beyond what has been said, to verify the accuracy of the proposed approach and to make it valid, the authors try to compare the proposed method against an analytical optimization method proposed by Palanichamy et al. [52,53] (see Appendix A).

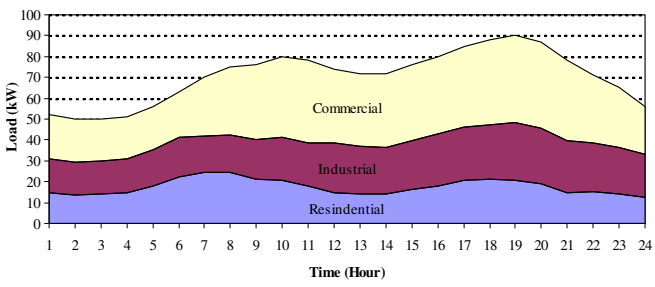

Fig. 7. Daily load curve in a typical Micro-Grid.

Table 4
The real-time market prices.

h	Price (€ct/kWh)
1	0.23
2	0.19
3	0.14
4	0.12
5	0.12
6	0.20
7	0.23
8	0.38
9	1.50
10	4.00
11	4.00
12	4.00
13	1.50
14	4.00
15	2.00
16	1.95
17	0.60
18	0.41
19	0.35
20	0.43
21	1.17
22	0.54
23	0.30
24	0.26

Table 5
Installed DG sources.

ID	Type	Min power (kW)	Max power (kW)
1	MT	6	30
2	PAFC	3	30
3	PV	0	25
4	WT	0	15
5	Bat	−30	30
6	Utility	−30	30

Table 6
Bids & emissions of the DG sources

ID	Type	Bid (€ct/kWh)	Start-up/ shut-down cost (€ct)	CO_2 (kg/MWh)	SO_2 (kg/MWh)	NO_x (kg/MWh)
1	MT	0.457	0.96	720	0.0036	0.1
2	PAFC	0.294	1.65	460	0.003	0.0075
3	PV	2.584	0	0	0	0
4	WT	1.073	0	0	0	0
5	Batt	0.38	0	10	0.0002	0.001

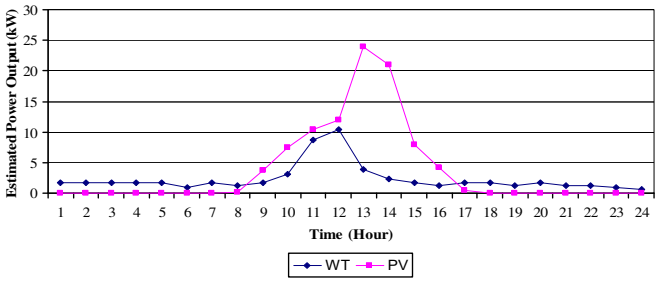

Fig. 8. Forecasted power outputs from RESs.

Table 7
Forecasting output of WT & PV.

h	WT (kW)/installed (kW)	PV (kW)/installed (kW)
1	0.119	0
2	0.119	0
3	0.119	0
4	0.119	0
5	0.119	0
6	0.061	0
7	0.119	0
8	0.087	0.008
9	0.119	0.150
10	0.206	0.301
11	0.585	0.418
12	0.694	0.478
13	0.261	0.956
14	0.158	0.842
15	0.119	0.315
16	0.087	0.169
17	0.119	0.022
18	0.119	0
19	0.0868	0
20	0.119	0
21	0.0867	0
22	0.0867	0
23	0.061	0
24	0.041	0

8.1. First scenario (Main Case)

In the first scenario it's assumed that all DGs with related characteristics produce electricity within the MG and additional demand or surplus of energy inside the grid is exchanged with the utility from the point of common coupling (PCC). All the units including the macro-gird (utility) can operate just within their power limits while satisfying the needed constraints. Performance evaluation of several optimization algorithms along with their best results in the case of each objective is presented in Tables 8 and 9 respectively.

Table 8
Comparison of results in the case of cost objective for 20 trials (*Main Case*).

Type	Best solution (€ct)	Worst solution (€ct)	Average (€ct)	Standard deviation (€ct)
GA	162.9469	198.5134	179.6502	24.5125
PSO	162.0083	180.2282	171.2103	12.6034
FSAPSO	161.5561	175.5402	168.2442	10.0025
CPSO-T	161.0580	165.3110	162.9845	2.9971
CPSO-L	160.7708	163.5512	162.1614	1.9660
AMPSO-T	159.9244	160.4091	160.2368	0.3427
AMPSO-L	159.3628	159.6813	159.5143	0.0963

Table 9
Comparison of results in the case of emission objective for 20 trials (*Main Case*).

Type	Best solution (kg)	Worst solution (kg)	Average (kg)	Standard deviation (kg)
GA	435.2363	457.4680	445.3862	14.2299
PSO	435.8227	454.5917	445.1072	13.9708
FSAPSO	435.0830	451.3821	443.4396	11.3525
CPSO-T	434.9973	444.9398	440.1036	6.9950
CPSO-L	434.9354	443.6383	439.2369	6.1538
AMPSO-T	434.8611	435.1126	434.9983	0.1786
AMPSO-L	434.8193	435.0099	434.9235	0.0681

In these tables, all the evolutionary optimization methods including the GA, PSO, FSAPSO, CPSO-T (Chaotic PSO based on Tent equation), CPSO-L (Chaotic PSO based on Logistic equation), AMPSO-L (Adaptive Modifies PSO based on Logistic equation) and AMPSO-T (Adaptive Modified PSO based on Tent equation) are compared for 20 random trials for both objective functions. For better understanding of the AMPSO performance, the convergence characteristics of AMPSO-L against the standard PSO algorithm for the best solution and in the case of each objective are shown in Figs. 9 and 10 separately. Likewise, the best optimal power allocations to the DGs using the proposed algorithm (AMPSO-L) are

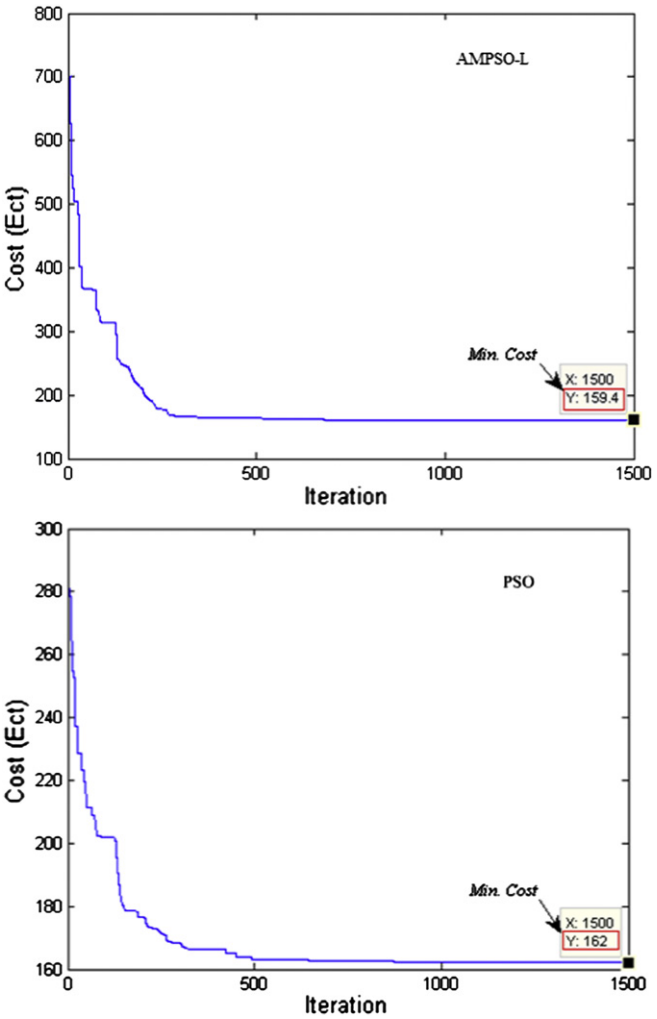

Fig. 9. Convergence characteristics of AMPSO-L and PSO in the case of cost objective (*main scenario*).

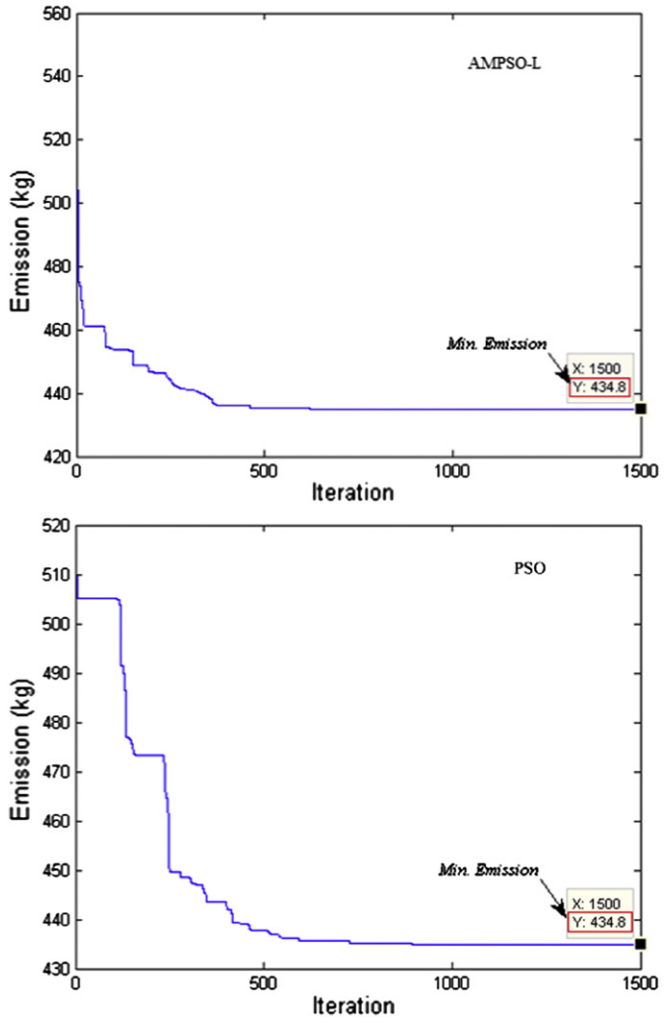

Fig. 10. Convergence characteristics of AMPSO-L and PSO in the case of emission objective (*main scenario*).

Table 10
Economic power dispatch using AMPSO-L (*Main Case*: Total cost = 156.3628 €ct).

Time (h)	Units					
	MT (kW)	FC (kW)	PV (kW)	WT (kW)	Batt (kW)	Utility (kW)
1	6.0879	28.741	0	0	−10.553	27.7236
2	6	14.4023	0	0.0005	−0.1090	29.7062
3	6	15.4825	0	0	−1.4739	29.9915
4	6	12.545	0	0.0002	2.4548	30
5	6.1626	17.495	0	0	2.4661	29.8763
6	6.5555	29.1178	0	0	−2.6667	29.9934
7	6	22.3893	0	0	12.3333	29.2773
8	6.0292	29.5403	0	0	23.2481	16.1824
9	29.9836	29.9985	0.0168	1.7855	29.9792	−15.7637
10	30	30	7.4938	3.0815	29.9993	−20.5746
11	29.994	30	9.2913	8.707	30	−29.9923
12	30	30	3.5586	10.399	30	−29.9577
13	29.9803	30	0.0159	3.7738	30	−21.77
14	29.9963	30	9.5516	2.3766	30	−29.9245
15	29.9998	29.9936	0.0871	1.7855	30	−15.866
16	29.9981	29.98	0	1.2714	30	−11.2495
17	29.4817	29.9514	0.0052	0	29.978	−4.4164
18	6	29.9154	0	0.0199	29.8365	22.2282
19	6.0059	29.8798	0	0.0037	27.4502	26.6604
20	6	29.9901	0	0	29.9981	21.0118
21	30	30	0	1.2033	30	−13.2033
22	29.9616	29.6838	0	0.0049	29.9257	−18.576
23	6.0031	14.6298	0	0	29.1347	15.2324
24	6.1143	4.8857	0	0	15	30

Table 11
Environmental power dispatch using AMPSO-L (*Main Case*: Total emission = 434.8193 kg).

Time (h)	Units					
	MT (kW)	FC (kW)	PV (kW)	WT (kW)	Batt (kW)	Utility (kW)
1	6.0024	30	0	1.78554	15	−0.7879
2	6	30	0	1.78554	30	−17.785
3	6.0065	30	0	1.78554	30	−17.792
4	6.0118	30	0	1.78554	30	−16.797
5	6.0024	30	0	1.78554	29.9999	−11.787
6	6	30	0	0.91324	29.9982	−3.9115
7	6	30	0	1.78554	30	2.21445
8	6	30	0.19374	1.30166	30	7.50459
9	6	29.9896	3.75395	1.78554	30	4.47090
10	6	30	7.52793	3.08541	29.9999	3.38667
11	6	30	10.4411	8.77236	30	−7.21354
12	6	30	11.9640	10.4132	30	−14.3773
13	6	30	23.8929	3.92283	29.9999	−21.8158
14	6	30	21.0493	2.37655	29.9995	−17.4255
15	6	30	7.86474	1.78549	29.9989	0.35078
16	6.0060	30	4.22076	1.30166	30	8.47153
17	6	30	0.53879	1.78554	30	16.6756
18	6	30	0	1.78554	30	20.2144
19	6	30	0	1.30166	30	22.6983
20	6	30	0	1.78554	30	19.2144
21	6.0034	30	0	1.30166	29.9998	10.6949
22	6.0036	30	0	1.30166	30	3.69469
23	6	30	0	0.91203	30	−1.91203
24	6	30	0	0.61244	30	−10.6124

presented in Tables 10 and 11 regarding each objective function minimization. Comparison of results in the case of best and worst solutions for both objectives indicates that the proposed AMPSO-L algorithm not only demonstrates a better performance but also presents a faster convergence characteristic. Moreover, the statistical indices of average and standard deviation confirm another advantage of the proposed algorithm in optimization process. It can be also seen from Figs. 9 and 10 that the cost objective function value reaches to minimum after 681 iterations with AMPSO-L method and does not vary thereafter while the PSO algorithm converges in 870 iterations. Similarly the value of emission objective function settles to the minimum in 619 iterations with AMPSO-L method, while the PSO algorithm converges in 891 iterations. Besides, the numerical results of multi-objective operation obtained by the proposed AMPSO-L algorithm indicate that in the first hours of the day a large portion of the load is supplied by the FC within the grid and the utility through the PCC because the bids of corresponding units are lower in comparison with those of others during the examined period. Due to growth of demand and bids of utility during the next hours of the day DGs increase their output powers according to priority in lower cost and emission correspondingly. It should be also noted that the charging process of the NiMH-Battery is done at the first hours of the day when the prices are low but the discharge action is postponed to the midday when

Table 12
Comparison of results in the case of cost objective for 20 trials (*Max-Renw*).

Type	Best solution (€ct)	Worst solution (€ct)	Average (€ct)	Standard deviation (€ct)
GA	277.7444	304.5889	290.4321	13.4421
PSO	277.3237	303.3791	288.8761	10.1821
FSAPSO	276.7867	291.7562	280.6844	8.3301
CPSO-T	275.0455	286.5409	277.4045	6.2341
CPSO-L	274.7438	281.1187	276.3327	5.9697
AMPSO-T	274.5507	275.0905	274.9821	0.3210
AMPSO-L	274.4317	274.7318	274.5643	0.0921

Table 13
Comparison of results in the case of emission objective for 20 trials (*Max-Renw*).

Type	Best solution (kg)	Worst solution (kg)	Average (kg)	Standard deviation (kg)
GA	435.1308	448.7740	441.2402	5.2689
PSO	435.5555	438.2212	436.5928	1.2666
FSAPSO	435.0037	437.1788	436.0913	1.5380
CPSO-T	434.9814	436.9001	435.9408	1.3567
CPSO-L	434.9064	436.3830	435.6447	1.0441
AMPSO-T	434.8611	435.0102	434.9357	0.1054
AMPSO-L	434.8161	434.9690	434.8920	0.0586

Table 14
Economic power dispatch using AMPSO-L (*Max-Renw*: Total cost = 274.4317 €ct).

Time (h)	Units					
	MT (kW)	FC (kW)	PV (kW)	WT (kW)	Batt (kW)	Utility (kW)
1	6	28.8862	0	1.7855	−14.671	30
2	6	21.5035	0	1.7855	−9.2891	30
3	6	26.4814	0	1.7855	−14.266	30
4	6	29.993	0	1.7855	−16.778	30
5	6	26.6394	0	1.7855	−8.424	30
6	6	29.9993	0	0.9142	−3.913	30
7	6	23.4284	0	1.7855	8.7861	30
8	6	30	0.1937	1.3017	23.784	13.7198
9	30	30	3.754	1.7855	30	−19.5395
10	30	30	7.5279	3.0854	30	−20.6133
11	28.7865	29.9999	10.4412	8.7724	30	−30
12	21.6227	30	11.964	10.4133	30	−30
13	14.1839	29.9999	23.8934	3.9228	30	−30
14	18.5741	30	21.0493	2.3766	30	−30
15	30	30	7.8647	1.7855	30	−23.6503
16	30	30	4.2208	1.3017	30	−15.5224
17	30	30	0.5389	1.7855	30	−7.3244
18	6	30	0	1.7855	30	20.2145
19	6.0002	30	0	1.3017	29.999	22.6983
20	6	30	0	1.7855	30	19.2145
21	30	30	0	1.3017	30	−13.3017
22	28.6036	30	0	1.3017	30	−18.9052
23	6	30	0	0.9142	15.192	12.8935
24	6	18.2558	0	0.6124	1.1318	30

Table 15
Comparison of results in the case of cost objective for 20 trials (*Inf-Eneg.Exch*).

Type	Best solution (€ct)	Worst solution (€ct)	Average (€ct)	Standard deviation (€ct)
GA	91.3293	127.7625	105.2070	13.4005
PSO	90.7629	112.8628	99.8493	10.8689
FSAPSO	90.6919	108.7761	99.7340	9.7874
CPSO-T	90.5545	102.1001	96.3273	8.1639
CPSO-L	90.4833	100.8786	95.6809	7.3505
AMPSO-T	89.9917	90.6221	90.3119	0.4457
AMPSO-L	89.9720	90.0431	90.0080	0.0921

Table 16
Comparison of results in the case of emission objective for 20 trials (*Inf-Eneg.Exch*).

Type	Best solution (kg)	Worst solution (kg)	Average (kg)	Standard deviation (kg)
GA	435.9708	458.6008	447.3231	7.0154
PSO	434.8319	448.7398	440.9284	4.8683
FSAPSO	434.8287	438.2267	436.0913	2.3211
CPSO-T	434.8263	437.0801	435.9408	1.5534
CPSO-L	434.8204	436.9937	435.6447	1.5309
AMPSO-T	434.8190	435.0100	434.9357	0.1350
AMPSO-L	434.8168	434.9998	434.9038	0.0604

Table 17
Economic power dispatch using AMPSO-L (*Inf-Eneg.Exch*: Total cost = 89.9720 €ct).

Time (h)	Units					
	MT (kW)	FC (kW)	PV (kW)	WT (kW)	Batt (kW)	Utility (kW)
1	6.0061	3.0023	0	0	−15	57.9916
2	6.0021	3.0065	0	0	−29.9672	70.9585
3	6.0069	3.0059	0	0	−30	70.9872
4	6	3.0005	0	0	−29.999	71.9985
5	6	3.008	0	0.0009	−30	76.9911
6	6	3.0404	0	0	−18.7679	72.7275
7	6	3	0	0	−4.1048	65.1048
8	6.0004	29.9869	0	0	10.8885	28.1242
9	29.9994	30	0	1.7855	25.8884	−11.6734
10	30	30	7.5279	3.0853	30	−20.6132
11	29.9998	30	10.4412	8.7723	29.9994	−31.2127
12	29.9997	30	11.9623	10.4133	29.9996	−38.3749
13	29.9998	30	0	3.9228	30	−21.9226
14	30	30	21.0493	2.3766	30	−41.4258
15	30	30	0.0001	1.7836	30	−15.7837
16	30	30	0.0024	1.3017	30	−11.3041
17	29.9877	29.9999	0	0	30	−4.9876
18	6.0157	29.9998	0	0	29.9818	22.0027
19	6.0059	29.9844	0	0	29.9974	24.0123
20	6.0027	29.9998	0	0.0037	29.9999	20.9938
21	30	30	0	1.2777	30	−13.2777
22	30	30	0	0	30	−19
23	6	29.982	0	0	15	14.018
24	6	3	0	0	0.1042	46.8958

the load curve reaches peak values. From another point of view, although employing RESs such as wind and solar results less pollution inside the grid, it causes more cost in short-term operation, therefore exploitation of energy form such resources must be limited according to economical considerations.

8.2. Second scenario (Max-Renw)

In the second scenario it's assumed that RESs (WT & PV) are exploited at their available maximum power outputs during each hour of the day and the rests of DGs including MT, PAFC, NiMH-Battery and the utility act as in the main case. Again, the entire optimization schemes are applied to the optimization problem and corresponding results are recorded. Tables 12 and 13 show

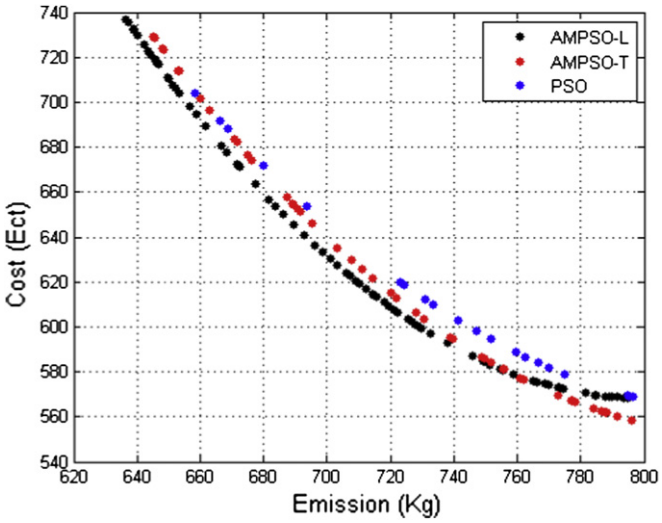

Fig. 11. Comparison of Emission and Cost Pareto-optimal front of AMPSO-L, AMPSO-T and PSO algorithms.

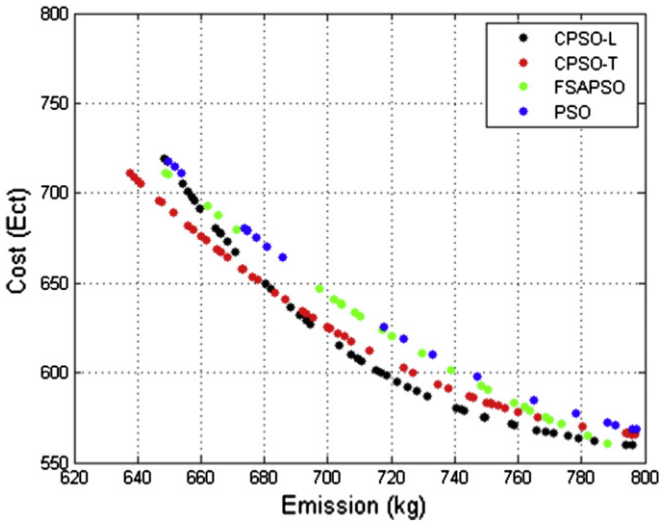

Fig. 12. Comparison of Emission and Cost Pareto-optimal front of CPSO-L, CPSO-T, FSAPSO and PSO algorithms.

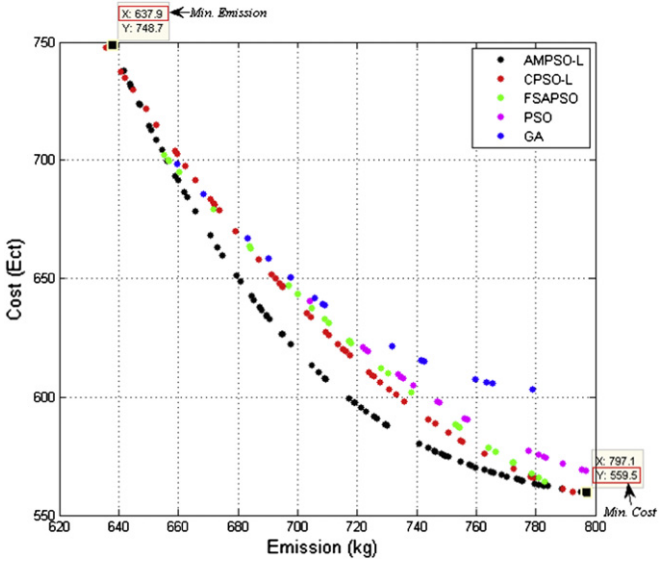

Fig. 13. Comparison of Emission and Cost Pareto-optimal front of all optimization algorithms.

brief comparisons from the performances of the mentioned algorithms regarding each objective for 20 trials. Similarly, the result of economic power dispatch using the proposed approach is indicated in Table 14. It should be mentioned that the results of environmental power dispatch don't vary greatly among the scenarios mainly due to the fact that all RESs (which have the lowest emissions) are utilized up to their extremes during the examined period.

Regarding the second scenario, it's again observed that the proposed algorithm allocates optimal power set points to the DGs appropriately while keeping small diversity in finding the optimal solutions during different trials in the case of each objective. It's also investigated from Table 14 that the operating cost of the MG increases greatly in comparison with the main case and demonstrates a growth of %75.5 in related cost. In other words, although higher penetration of RESs into the grid environment results lower emission, it imposes higher cost of operation.

8.3. Third scenario (Inf-Eneg.Exch)

In the last scenario, it's supposed that the utility behaves as an unconstraint unit and exchanges energy with the MG without any limitation while the rests of DGs and their related characteristics remain unchanged. Similar to the previous scenarios, all the optimization algorithms are implemented to solve the economic dispatch problem and the simulation results are gathered correspondingly as shown in Tables 15 and 16. The best performance of AMPSO-L in scheduling of the units for a day ahead and in terms of cost objective is also shown in Table 17. Once again, it's observed that the proposed algorithm can solve the optimization problem successfully while maintains small variations in finding optimal solutions considering both objectives. Moreover, the numerical results of Table 17 indicate that allocation of optimal powers to DGs regarding an unlimited power exchange situation ends in a reduction of %42.45 in operation cost of the MG in comparison with the main case. It's also notable that in the third scenario the utility takes the lead in supplying the load inside the grid during the first hours of the day while purchasing energy in bulk amount from the MG during the peak times. From an economical point of view, WT and PV start-up when shortage of power generation occurs inside the grid or there is a need for more energy export to the macro-grid. Likewise, other DGs such as FC, MT and NiMH-Battery adjust their generation set points according to load levels during each hour of the day in an economical manner.

Now to incorporate the availability of DGs in optimization scheme while considering both objectives, suitable ON (OFF) states (0/1) are assigned to DGs during the power dispatch process. In such situation, all the units are allowed to start-up or shut-down for the flexible operation of the MG while considering minimum cost and emission as competitive objectives. Again all the evolutionary methods are implemented to solve the multi-operation management problem and related results as well as the distribution of the Pareto-optimal sets over the trade-off surfaces are gathered truthfully. The fuzzy-based clustering procedure is also utilized to control the size of repository during the optimization process. In this regard, the Pareto-fronts for emission and cost objectives obtained by PSO, AMPSO-L and AMPSO-T algorithms are shown in Fig. 11. The comparison of Pareto-fronts obtained by CPSO-T, CPSO-L, FSAPSO and PSO are also illustrated in Fig. 12 respectively. Comparison of results in the case of Pareto-fronts for emission and cost objectives obtained by AMPSO-L, CPSO-L, FSAPSO, PSO and GA is also demonstrated in Fig. 13. In the same figure, the extreme points on the Pareto front obtained by the proposed algorithm are shown as examples of two non-dominated solutions with minimum emission-maximum cost and minimum cost-maximum emission, respectively. The schedules of multi-operation management regarding each mentioned situation are tabulated in Tables 18 and 19 separately.

It's observed from Fig. 11 that the non-dominated solutions achieved by the proposed AMPSO-L algorithms are well-distributed over the Pareto front although the one from standard PSO lacks this feature. Similarly, through comparison of results obtained by CPSO-T, CPSO-L, FSAPSO and PSO it's concluded that hybrid PSO approaches (e.g., FSAPSO or CPSO) improve the capability of a classic PSO in finding non-dominated solutions to a high extent although there are slight differences between their corresponding performances. It's also important to mention that the performances obtained by the AMPSO-L methods outweigh the ones from other algorithms both in terms of non-dominated solutions and diversity of them along the Pareto front as shown in Fig. 13.

Table 18
Multi-operation management using AMPSO-L (Minimum emission/maximum cost: Total cost = 637.9021 €ct, Total emission = 748.731 kg).

Time (h)	DG Units											
	State						Output power					
	MT	FC	PV	WT	Batt	Utility	MT (kW)	FC (kW)	PV (kW)	WT (kW)	Batt (kW)	Utility (kW)
1	1	0	1	0	0	1	30	0	0	0	0	22
2	0	1	1	1	1	1	0	23.2516	0	1.2901	15	10.4582
3	0	1	1	1	1	0	0	24.4556	0	0.275	25.2694	0
4	1	1	0	1	1	1	12.7687	30	0	1.78554	30	−23.554
5	1	0	0	1	1	1	30	0	0	0.36763	30	−4.3676
6	1	1	1	1	1	1	30	22.8931	0	0.20483	21.3122	−11.410
7	0	1	1	1	1	1	0	30	0	0.43394	28.8520	10.7140
8	0	1	1	1	1	1	0	30	0.19375	1.30166	30	13.5046
9	0	1	0	1	1	1	0	30	0	1.78554	30	14.2145
10	1	1	0	1	1	1	30	30	0	3.08542	30	−13.085
11	0	1	1	1	1	0	0	28.7865	10.4412	8.77237	30	0
12	1	1	0	1	1	1	9.2932	30	0	10.4133	30	−5.7065
13	1	0	1	1	1	1	21.3074	0	5.14984	1.04588	28.0076	16.4893
14	1	1	1	1	1	1	15.9401	30	14.7868	2.37656	30	−21.103
15	1	0	0	0	1	1	16	0	0	0	30	30
16	0	1	1	1	1	1	0	30	4.22077	1.30166	27.0698	17.4078
17	0	1	0	0	1	1	0	30	0	0	30	25
18	1	0	1	1	1	1	30	0	0	1.78554	26.2145	30
19	0	1	1	1	1	1	0	28.6983	0	1.3017	30	30
20	0	1	1	0	1	1	0	27	0	0	30	30
21	1	0	1	1	1	1	30	0	0	1.3017	28.8964	17.8019
22	1	1	0	1	1	0	30	14.8867	0	1.3017	24.8116	0
23	1	1	1	0	1	0	7.8492	27.1508	0	0	30	0
24	0	1	0	0	1	0	0	30	0	0	26	0

Table 19
Multi-operation management using AMPSO-L (Minimum cost/maximum emission: Total cost = 559.4872 €ct, Total emission = 797.1101 kg).

Time (h)	DG Units											
	State						Output Power					
	MT	FC	PV	WT	Batt	Utility	MT (kW)	FC (kW)	PV (kW)	WT (kW)	Batt (kW)	Utility (kW)
1	1	1	0	1	1	0	30	5.2144	0	1.7855	15	0
2	1	1	1	0	1	1	20.726	3	0	0	22.051	4.2225
3	1	0	0	1	1	0	29.7902	0	0	0.5660	19.6436	0
4	0	1	1	1	1	0	0	19.4532	0	1.7855	29.7612	0
5	1	0	1	0	1	0	26	0	0	0	30	0
6	1	1	0	1	1	0	17.8923	30	0	0.1077	15	0
7	1	1	1	1	1	1	30	3	0	1.7855	16.92362	18.2908
8	0	1	1	1	1	1	0	30	0.1247	1.3017	13.5735	30
9	1	1	0	1	1	0	30	17.2657	0	0.1607	28.5735	0
10	1	1	0	0	1	1	28.7951	30	0	0	21.2048	0
11	1	1	1	0	1	1	30	30	10.4411	0	30	−22.4412
12	1	1	1	0	1	1	30	30	11.9640	0	30	−27.964
13	1	0	0	1	1	1	30	0	0	0.1287	30	11.8712
14	1	1	1	0	1	1	28.3006	30	5.6980	0	30	−21.9987
15	1	1	1	1	1	1	30	19.2424	0.0785	0.9922	25.6868	0
16	1	1	1	0	1	1	20.2427	29.5252	1.0080	0	11.1615	18.0623
17	1	1	1	1	0	1	30	30	0.5389	1.7855	0	22.6755
18	1	1	0	1	1	1	24.3746	30	0	1.7855	15	16.8397
19	1	1	1	1	0	1	28.6983	30	0	1.3017	0	30
20	1	1	1	1	1	1	30	13.2532	0	0	15	28.7467
21	1	1	1	1	0	1	30	17.3224	0	0.6776	0	30
22	1	0	1	1	1	1	30	0	0	0	15	26
23	1	0	0	0	1	1	6	0	0	0	30	29
24	1	1	1	0	1	1	6	21.4939	0	0	30	−1.4939

9. Conclusion

In this paper, an expert multi-objective Adaptive Modified PSO (AMPSO) optimization algorithm is proposed and implemented to solve the multi-operation management problem in a typical MG with RESs. A CLS approach is applied to find the best local solutions within the search space and a FSA mechanism is utilized to adjust PSO parameters when they are needed. Moreover, a fuzzy clustering approach is used to control the size of repository for non-dominated solutions. To evaluate the performance of the proposed algorithm several test cases are introduced and the simulation results are gathered subsequently. The numerical results indicate that the proposed method not only demonstrates superior performances but also shows dynamic stability and excellent convergence of the swarms. The proposed method also yields a true and well-distributed set of Pareto-optimal solutions giving the system operators various options to select an appropriate power dispatch plan according to environmental or economical considerations.

Appendix A

To compare the performance of the proposed algorithm with some analytical methods a test system with three plants and six generating units is considered as shown in Fig. A.1. The fuel costs and the emission coefficients of corresponding units are tabulated in Tables A.1–A.2. For simplicity, only one type of pollutant (NO_x) is considered for optimization process. The transmission loss coefficients are also shown in (A.1). More information on related test system is given in Ref. [52].

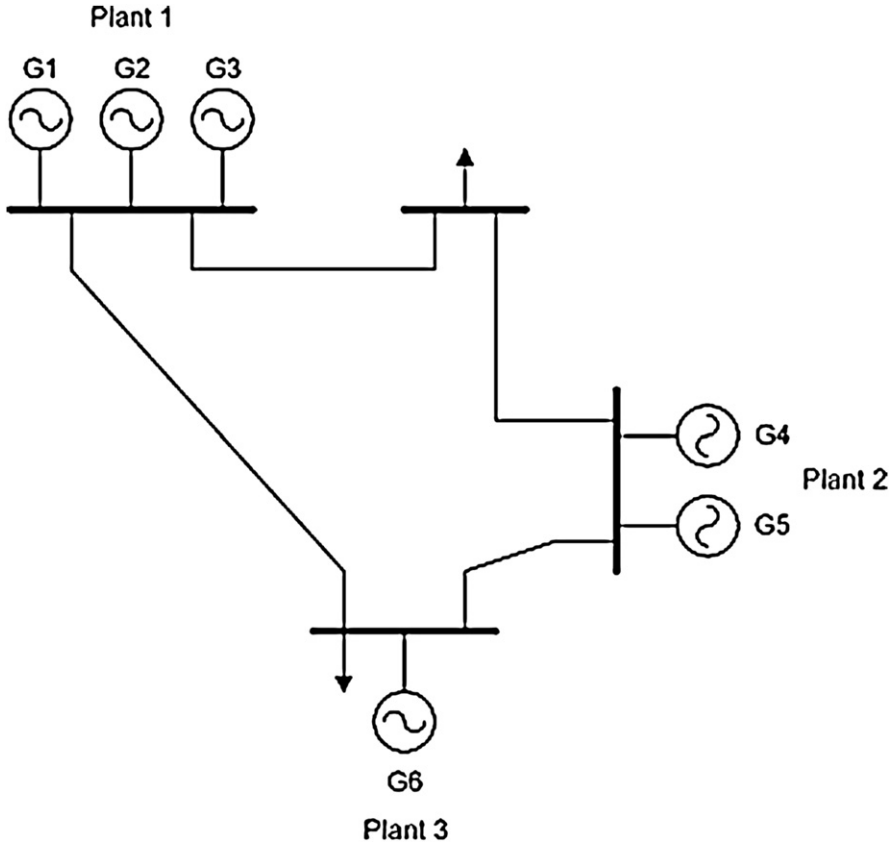

Fig. A.1. A Typical 4-bus test system with six generation units [52].

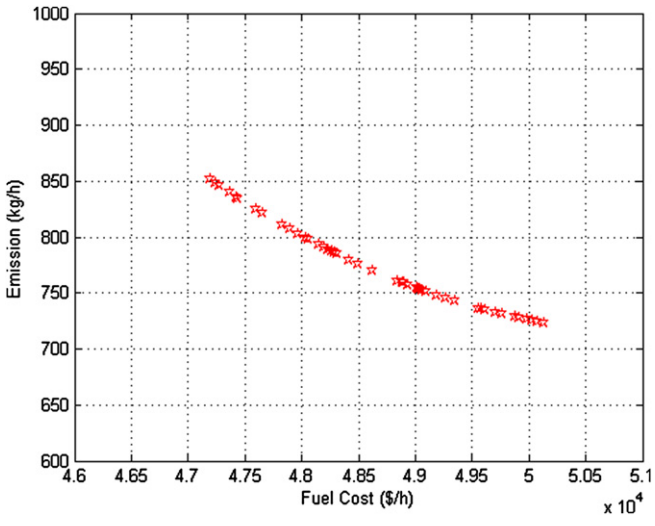

Fig. A.2. Pareto-fronts of AMPSO algorithm for the test system.

Table A.1
Fuel cost coefficients.

Plant	Unit	Fuel cost coefficients			$P_{G,\min}$ (MW)	$P_{G,\max}$ (MW)
		a_i	b_i	c_i		
1	G_1	0.15274	38.53973	756.79886	10	125
	G_2	0.10578	46.15916	451.32513	10	150
	G_3	0.02803	40.39655	1049.32513	40	250
2	G_4	0.03546	38.30553	1243.5311	35	210
	G_5	0.02111	36.32782	1658.5696	130	325
3	G_6	0.01799	38.27041	1356.65920	125	315

Table A.2
Emission coefficients (NO_x).

Plant	Unit	Fuel cost coefficients			$P_{G,\min}$ (MW)	$P_{G,\max}$ (MW)
		d_i	e_i	f_i		
1	G_1	0.00419	0.32767	13.85932	10	125
	G_2	0.00419	0.32767	13.85932	10	150
	G_3	0.00683	−0.54551	40.2669	40	250
2	G_4	0.00683	−0.54551	40.2669	35	210
	G_5	0.00461	−0.51116	42.89553	130	325
3	G_6	0. 00461	−0.51116	42.89553	125	315

Table A.3
Simulation results for economic dispatch.

Optimization method	AMPSO	Ref. [52]	Ref. [53]
P_1(MW)	33.71	33.77	33.77
P_2(MW)	12.65	12.65	12.65
P_3(MW)	150.54	150.57	150.56
P_4(MW)	148.5	148.50	148.50
P_5(MW)	296.32	296.29	296.29
P_6(MW)	293.71	293.69	293.68
Total cost ($/h)	47187.36	47188.38	47188.29
Net emission (kg/h)	857.79	857.76	857.74
Total loss (MW)	35.43	35.46	35.45
CPU time (s)[a]	10.35	0.805	0.189

[a] The results are on an Intel Pentium III processor, 996 MHz, 416 MB of RAM computer.

Table A.4
Simulation results for emission dispatch.

Optimization method	AMPSO	Ref. [52]	Ref. [53]
P_1(MW)	124.51	124.53	124.51
P_2(MW)	124.51	124.53	124.51
P_3(MW)	140.306	140.32	140.31
P_4(MW)	140.306	140.32	140.31
P_5(MW)	204.14	204.16	204.15
P_6(MW)	204.14	204.16	204.15
Total cost ($/h)	50217.47	50223.26	50217.62
Net emission (kg/h)	696.91	697.06	696.99
Total loss (MW)	37.91	38.02	37.92
CPU time (s)	10.33	0.805	0.189

Table A.5
Simulation results for economic/emission dispatch.

Optimization method	AMPSO	Ref. [52]	Ref. [53]
P_1(MW)	51.82	51.83	51.82
P_2(MW)	32.65	38.66	38.64
P_3(MW)	208.77	248.74	248.73
P_4(MW)	128.12	122.15	122.14
P_5(MW)	292.03	252.03	252.02
P_6(MW)	223.57	223.58	223.57
Total cost ($/h)	47548.97	47809.03	47804.55
Net emission (kg/h)	823.35	843.53	843.42
Total loss (MW)	36.89	36.99	36.90
CPU time (s)	12.54	0.814	0.195

$$B_{ij} = \begin{bmatrix} 0.000091 & 0.000031 & 0.000029 \\ 0.000031 & 0.000062 & 0.000028 \\ 0.000029 & 0.000028 & 0.000072 \end{bmatrix} \quad \text{(A.1)}$$

Tables A.3–A.5 provide the dispatch results of the proposed and the classical methods in the case of economic dispatch, emission dispatch and combined economic and emission dispatch with transmission losses, respectively. For the entire test cases the load demand is fixed to 900 MW. As observed from numerical results, the proposed AMPSO not only demonstrates better results in the case of each single objective but also outweighs in optimal power dispatch regarding both objectives compared to the conventional analytical methods mentioned in Refs. [52,53]. The Pareto-fronts of AMPSO algorithm in the case of both objectives is also shown in Fig. A.2 for the mentioned test system. As an example, it's observed that by applying AMPSO to optimal power dispatch problem the total cost reduces about 1.02 ($/h) in comparison with the one proposed in Ref. [52] and about 0.93 ($/h) compared to the Ref. [53] regarding the cost objective. Likewise, the net emission inside the grid reduces 0.15 (kg/h) and 0.8 (kg/h) by using the AMPSO algorithm in comparison with Refs. [52,53] considering emission objective solely.

References

[1] Ayres RU, Turton H, Casten T. Energy efficiency, sustainability and economic growth. Energy 2007;32(5):634–48.
[2] Sanseverino ER, Di Silvestre ML, Ippolito MG, De Paola A, Re GL. An execution, monitoring and replanning approach for optimal energy management in micro grids. Energy 2011;36(5):3429–36.
[3] Niknam T, Zeinoddini Meymand H, Doagou Mojarrad H. An efficient algorithm for multi-objective optimal operation management of distribution network considering fuel cell power plants. Energy 2011;36(1):119–32.
[4] Houwing M, Ajah AN, Heijnen PW, Bouwmans I, Herder PM. Uncertainties in the design and operation of distributed energy resources: the case of micro-CHP systems. Energy 2008;33(10):1518–36.
[5] Pearce JM. Expanding photovoltaic penetration with residential distributed generation from hybrid solar photovoltaic and combined heat and power systems. Energy 2009;34(11):1947–54.
[6] Hawkes AD, Leach MA. Cost-effective operating strategy for residential micro-combined heat and power. Energy May 2007;32(5):711–23.
[7] Dali M, Belhadj J, Roboam X. Hybrid solar–wind system with battery storage operating in grid-connected and standalone mode: control and energy management – experimental investigation. Energy 2010;35(6):2587–95.
[8] Pouresmaeil E, Montesinos-Miracle D, Gomis-Bellmunt O, Bergas-Jané J. A multi-objective control strategy for grid connection of DG (distributed generation) resources. Energy 2010;35(12):5022–30.
[9] Sayyaadi H, Babaie M, Farmani MR. Implementing of the multi-objective particle swarm optimizer and fuzzy decision-maker in exergetic, exergoeconomic and environmental optimization of a benchmark cogeneration system. Energy 2011;36(8):4777–89.
[10] Wood AJ, Wollenberg BF. Power generation, operation and control. New York: Wiley; 1984.
[11] Talaq JH, El-Hawary F, El-Hawary ME. A summary of environmental/economic dispatch algorithms. IEEE Trans Power Syst 1994;9:1508–16.
[12] Gent MR, Lamont JW. Minimum emission dispatch. IEEE Trans Power Apparatus Syst 1971;90:2650–60.
[13] Coello CAC. A comprehensive survey of evolutionary-based multiobjective optimization techniques. Knowledge and Information Systems 1999;1(3):269–308.
[14] Liao GC. A novel evolutionary algorithm for dynamic economic dispatch with energy saving and emission reduction in power system integrated wind power. Energy 2011;36(2):1018–29.
[15] Chen PH, Chang HC. Large-scale economic dispatch by genetic algorithm. IEEE Trans Power Syst 1995;10(4):1919–26.
[16] Park JB, Lee KS, Shin JR, Lee KY. A particle swarm optimization for economic dispatch with nonsmooth cost function. IEEE Trans Power Syst 2005;20(1):34–42.
[17] Sun J, Fang W, Wang D, Xua W. Solving the economic dispatch problem with a modified quantum-behaved particle swarm optimization method. Energ Convers Manage 2009;50(12):2967–75.
[18] Lin WM, Cheng FS, Tsay MT. Nonconvex economic dispatch by integrated artificial intelligence. IEEE Trans Power Syst 2001;16(2):307–11.
[19] Haung CM, Yang H, Huang CL. Bi-objective power dispatch using fuzzy satisfaction-maximizing decision approach. IEEE Trans Power Syst 1997;12(4):1715–21.
[20] Wong KP, Yuryevich J. Evolutionary programming based algorithm for environmentally constrained economic dispatch. IEEE Trans Power Syst 1998;13(2):301–8.
[21] Brar YS, Dhillon JS, Kothari DP. Multi-objective load dispatch based on genetic-fuzzy techniques. In: Power system conference and exposition, Oct. 29th–Nov 1; 2006. p. 931–936.
[22] Abido MA. A niched pareto genetic algorithm for multi objective environmental/economic dispatch. Int J Electr Power Energ Syst 2003;25:97–105.
[23] Senjyu T, Shimabukuro K, Uezato K, Funabashi T. A fast technique for unit commitment problem by extended priority list. IEEE Trans Power Syst 2003;18(2):882–8.
[24] Cohen AI, Yoshimura M. A branch-and-bound algorithm for unit commitment. IEEE Trans Power Apparatus Syst 1983;102:444–51.
[25] Ouyang Z, Shahidehpour SM. An intelligent dynamic programming for unit commitment application. IEEE Trans Power Syst 1991;6(3):1203–9.
[26] Lauer GS, Bertsekas Jr DP, Sandell NR, Posbergh TA. Solution of large-scale optimal unit commitment problems. IEEE Trans Power Apparatus Syst; 1982:79–86. PAS-101.
[27] Svoboda AJ, Tseng CL, Li CA, Johnson RB. Short-term resource scheduling with ramp constraints [power generation scheduling]. IEEE Trans Power Syst 1997;12(1):77–83.
[28] Lee FN. A fuel-constrained unit commitment method. IEEE Trans Power Syst 1989;4(3):1208–18.
[29] Virmani S, Adrian EC, Imhof K, Mukherjee S. Implementation of a Lagrangian relaxation based unit commitment problem. IEEE Trans Power Syst 1989;4(4):1373–80.
[30] Zhuang F, Galiana FD. Towards a more rigorous and practical unit commitment by Lagrangian relaxation. IEEE Trans Power Syst 1988;3(2):763–73.
[31] Peterson WL, Brammer SR. A capacity based Lagrangian relaxation unit commitment with ramp rate constraints. IEEE Trans Power Syst 1995;10(2):1077–84.

[32] Damousis IG, Bakirtzis AG, Dokopoulos PS. A solution to the unit-commitment problem using integer-coded genetic algorithm. IEEE Trans Power Syst 2004; 19(2):1165–72.
[33] Senjyu T, Saber AY, Miyagi T, Shimabukuro K, Urasaki N, Funabashi T. Fast technique for unit commitment by genetic algorithm based on unit clustering. IEE Proc Generat Transmission Distrib 2005;152(5):705–13.
[34] Cheng CP, Liu CW, Liu CC. Unit commitment by Lagrangian relaxation and genetic algorithms. IEEE Trans Power Syst 2000;15(2):707–14.
[35] Kazarlis SA, Bakirtzis AG, Petridis V. A genetic algorithm solution to the unit commitment problem. IEEE Trans Power Syst 1996;11(1):83–92.
[36] Kennedy J, Eberhart R. Particle swarm optimization. In: Proc. IEEE Int. Conf. Neural Networks (ICNN'95), vol. 4; 1995.
[37] Coello CA, Lechuga Mopso MS. A proposal for multi objective particle swarm optimization. In: Proceedings of IEEE world congress on computational intelligence; 2002. p. 1051–1056.
[38] Deb K, Thiele L, Laumanns M, Zitzler E. Scable multi-objective optimization test problems, In: Proceeding of IEEE world congress on computational intelligence (CEC2002); 2002.
[39] Fieldsend JE, Singh S. A multi objective algorithm based upon particle swarm optimization an efficient data structure on turbulence. In the 2002 U.K. workshop on computational Intelligence;2002. p. 34–44.
[40] Hu Eberhart X. Multi-objective optimization using dynamic nighbourhood particle swarm optimization. In: Proceedings of IEEE world congress on computational intelligence; 2002. p. 1677–1681.
[41] Mostaghim S, Teich J. Strategies for finding good local guides in multi-objective particle swarm optimization. In: Proc. of IEEE swarm intelligence symposium; 2003. p. 26–33.
[42] Hernandez-Aramburo CA, Green TC, Mugniot N. Fuel consumption minimization of a microgrid. IEEE Trans Ind Appl 2005;41(3).
[43] Conti S, Rizzo SA. Optimal control to minimize operating costs and emissions of MV autonomous micro-grids with renewable energy sources, Clean Electrical Power ICCEP'09; 2009. p. 634–639.
[44] Lin CM, Gen M. Multi-criteria human resource allocation for solving multistage combinatorial optimization problems using multiobjective hybrid genetic algorithm. Expert Syst Appl 2008;34:2480–90.
[45] Chang PC, Chen SH, Liu CH. Sub-population genetic algorithm with mining gene structures for multiobjective flowshop scheduling problems. Expert Syst Appl 2007;33:762–71.
[46] Wang L, Singh Ch. Environmental/economic power dispatch using fuzzified multi-objective particle swarm optimization algorithm. Electr Power Syst Res 2007;77:1654–64.
[47] Kalogirou SA. Artificial intelligence for the modeling and control of combustion processes: a review. Progr Energ Combust Sci 2003;29: 515–66.
[48] Kennedy J, Eberhart R. Particle swarm optimization. In: IEEE international conf. on neural networks. Piscataway, NJ, vol. 4; 1995. p. 1942–1948.
[49] Kennedy J, Eberhart RC. A discrete binary version of the particle swarm algorithm. In: Proc. IEEE conf. on systems, man, and cybernetics; 1997. p. 4104–4109.
[50] Liu B, Wang L, Jin YH, Tang F, Huang DX. Improved particle swarm optimization combined with chaos. Chaos Solitons Fractals 2005;25(5): 1261–71.
[51] Coelho LDS. A quantum particle swarm optimizer with chaotic mutation operator. Chaos Solitons Fractals 2008;37(5):1409–18.
[52] Palanichamy C, Srikrishna K. Economic thermal power dispatch with emission constraint. J Indian Inst Eng (India) 1991;72(11).
[53] Palanichamy C, Babu NS. Analytical solution for combined economic and emissions dispatch. Electr Power Syst Res 2008;78(7):1129–39.